# Artificial Neural Network modeling of a hydrogen dual fueled diesel engine characteristics: An experiment approach

**Article** *in* International Journal of Hydrogen Energy · May 2017

DOI: 10.1016/j.ijhydene.2017.04.096

CITATIONS
46

READS
664

**6 authors**, including:

Javed Syed
King Khalid University
**32** PUBLICATIONS **338** CITATIONS
SEE PROFILE

Rahmath Ulla Baig
King Khalid University
**30** PUBLICATIONS **269** CITATIONS
SEE PROFILE

Salem Algarni
King Khalid University
**75** PUBLICATIONS **914** CITATIONS
SEE PROFILE

Mohammad Masood
LORDS Institute of Engineering and Technology
**17** PUBLICATIONS **422** CITATIONS
SEE PROFILE

INTERNATIONAL JOURNAL OF HYDROGEN ENERGY XXX (2017) 1–25

Available online at www.sciencedirect.com

ScienceDirect

journal homepage: www.elsevier.com/locate/he

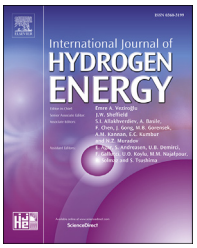

# Artificial Neural Network modeling of a hydrogen dual fueled diesel engine characteristics: An experiment approach

*Javed Syed* [a,*], *Rahmath Ulla Baig* [b], *Salem Algarni* [a], *Y.V.V. Satyanarayana Murthy* [c], *Mohammad Masood* [d], *Mohammed Inamurrahman* [e]

[a] *Department of Mechanical Engineering, College of Engineering, King Khalid University, Abha, Saudi Arabia*
[b] *Department of Mechanical Engineering, P.E.S Institute of Technology-South Campus, Bangalore, India*
[c] *Department of Mechanical Engineering, GITAM Institute of Technology, GITAM University, Visakhapatnam, India*
[d] *Department of Mechanical Engineering, Lords Institute of Engineering and Technology, Hyderabad, India*
[e] *Department of Computer Science, College of Sciences and Arts, King Khalid University, Dhahran Al Janoub, Saudi Arabia*

ARTICLE INFO

*Article history:*
Received 23 January 2017
Received in revised form
22 March 2017
Accepted 15 April 2017
Available online xxx

*Keywords:*
Hydrogen fuel
Artificial Neural Network
Diesel engine
Performance & emission characteristics
Emission–performance trade-off
Uncertainty analysis

ABSTRACT

The rapid growth of vehicular pollution; mostly running on the diesel engine, emissions emerging are the concerns of the day. Owing to clean burn characteristics features, Hydrogen ($H_2$) as a fuel is the paradigm of the researcher. Extensive research presented in the literature on $H_2$ dual fueled diesel engine reveals, the significant role of $H_2$ in reducing emissions and enhancing the performance of a dual fueled diesel engine. With meager qualitative experiment data, the feasibility to develop an efficient Artificial Neural Network (ANN) model is investigated, the developed model can be utilized as a tool to investigate the $H_2$ dual fueled diesel engine further. In the process of developing an ANN model, engine load and $H_2$ flow rate are varied to register performance and emission characteristics. The creditability of the experiment is ascertained with uncertainty analysis of measurable and computed parameters. Leave-out-one method is adopted with 16 data sets; seven training algorithms are explored with eight transfer function combinations to evolve a competent ANN model. The efficacy of the developed model is adjudged with standard benchmark statistic indices. ANN model trained with Broyden, Fletcher, Goldfarb, & Shanno (BFGS) quasi-Newton backpropagation (trainbfg) stand out the best among other algorithms with regression coefficient ranging between 0.9869 and 0.9996.



* *Corresponding author.*
E-mail address: syedjavedme@gmail.com (J. Syed).

http://dx.doi.org/10.1016/j.ijhydene.2017.04.096
0360-3199/

## Introduction

For decennaries, the dominant underpinning power source in industrial and transportation sector is diesel powered engines. With the rapid growth of transportation, emissions from the diesel-fueled engines are concerns of the day. Depletion of fossil fuel and an increase in emission made researchers endeavor for energy substitution with renewable and sustainable fuel in conjunction with a reduction in emissions. Literature divulges the cardinal role of hydrogen ($H_2$) as a dual fuel in diesel engines with enhanced performance and reduced emissions.

On the embarked prospect of performance enhancement and diminution in emission, the diesel engine was duel fueled with $H_2$. It was divulged that increase in $H_2$ energy substitution ratio increases thermal efficiency and $NO_x$ emissions [1]. Mathur et al. [2] investigated utilization of $H_2$ fuel in dual fueled diesel engine on a commercial 4 kW diesel engine. The $H_2$ flow rate of 20–50 l/min were attempted, water is injected as a diluent to the cylinder to reduce knocking at higher $H_2$ energy substitution. The significant findings of experimentation reiterate the fact that, $H_2$ could be expediently used to enhance performance and alleviate emissions.

$H_2$ induction through intake port was inquisited on Kirloskar AV-1 single cylinder diesel engine and compared outcomes with computational fluid dynamics analysis [3]. An increase in peak pressure & $NO_x$ emissions with advancement in ignition and increase in combustion velocity with the augmentation of $H_2$ substitution were reported. $H_2$ can be inducted into the cylinder by natural aspiration along with intake air or by injecting in the intake manifold. Lata et al. [4] inducted $H_2$ naturally through an intake manifold of a diesel engine running at 1500 rpm. At 80% engine load, $H_2$ dual fuel engine reported an increase in brake thermal efficiency (BTE) of 4.48% as compared to baseline diesel fuel, but $H_2$ flow rate beyond 45% energy substitution results in a decrease in BTE. In the presence of $H_2$ fuel, CO (carbon monoxide) emissions decrease as compared to baseline diesel fuel due to the absence of carbon particles.

An inquest into a variation of $H_2$ flow rate from 0 to 7.4% by energy was probed, $H_2$ substitution abates particulate matter emissions, and the effect of $H_2$ flow rate in reduction of $NO_x$ (nitrogen oxide) is marginal [5]. Santoso et al. [6] investigated $H_2$ addition at low engine load conditions; the engine was run at the constant speed of 2000 rpm and 10 Nm load. Enrichment of fuel mixture with $H_2$ flow rate from 21.4 to 49.6 l/min results in a decrease in peak pressure and BTE.

The role of $H_2$ energy substitution on engine performance and emissions is espied by De Morais et al. [7]. $H_2$ energy substitution was varied from 0 to 20% while varying engine load from 0 to 40 kW. It was found that small $H_2$ energy substitution results in a decrease in specific fuel consumption. Also, carbon dioxide emissions decrease with a supplement of $H_2$ fuel. With the increase in engine load, the oxygen concentration in exhaust decreases, whereas EGT increase. Zhou et al. [8] effectuated experiments by increasing $H_2$ energy substitution from 0 to 40% at a constant engine speed of 1800 rev/min. $H_2$ was naturally aspirated into the intake manifold, and engine load is varied. The role of $H_2$ energy substitution with engine load was apparent. With 30% $H_2$ energy substitution at 90% load, a drastic increase in peak pressure, shorten ignition delay and combustion duration was recorded. Results show erratic combustion at higher $H_2$ energy substitution operating at higher loads.

Owing to carbon-free characteristics of $H_2$ fuel along with high calorific value, emanating lower emissions and exhibiting better performance behavior, endeavors confirm utilization of $H_2$ as energy substitution as a dual fueled mode in a diesel engine with minor modifications to the existing diesel engine. On the other hand, $H_2$ dual fueled engine experimentations are strenuous and arduous. It is noteworthy to mention that, with minimum significant qualitative experimentation data, an efficient Artificial Neural Network (ANN) model can be modeled to accurately predict the performance and emission characteristics of a diesel engine running on diesel fuel [9–12]. Parlak et al. [9] designed backpropagation neural model with three inputs, seven neurons and two outputs (specific fuel consumption and EGT). The mean absolute relative error was employed to judge the efficacy of the model for a diesel engine. Yusaf et al. [10] model to predict diesel engine torque and emissions accede to regression coefficients of 0.955.

Uzan [11] illustrated the development of ANN model for a turbocharged inter cooled diesel engine. Predictions obtained with the well-trained model were used to perform parametric studies. Bietresato et al. [12] model to predict torque and brake specific fuel consumption (BSFC) of a diesel engine, various transfer functions were tested, and maximal regression coefficient was observed for Gaussian transfer functions.

Literature review reveals, $H_2$ has notable engine performance & emission characteristics and is viable to be used as dual fuel in a diesel engine. Numerous network models were developed for diesel engine running on diesel fuel. However, sparse ANN models were reported in the literature to predict performance and emission characteristics of an $H_2$ dual fueled diesel engine.

Current research aims at developing robust ANN model with meager data generated from the experiment, which can efficiently predict the performance and emission characteristics of $H_2$ dual fueled diesel engine. The efficacy of the developed model is adjudged comparing with the current experimental results adapting standard benchmark statistics indices. The developed model can aid in the further investigation of $H_2$ as a dual fuel in a diesel engine.

## Artificial Neural Network

Working model of ANN is quite close to the functioning of the human brain. When a set of input signal is received at a neuron, each input signal is weighted, sum together, and subjected to an activation (transfer) function. The neuron gets fired, i.e., transmit a signal to another neuron or environment when the resulted signal exceeds the threshold limit (bias) of the neuron. This configuration is known as a perceptron. The architecture of the perceptron is shown in Fig. 1.

The outcome of the perceptron is judged based upon the performance function such as Mean Squared Error (MSE). New weights and activation levels are redefined feeding the error.

Please cite this article in press as: Syed J, et al., Artificial Neural Network modeling of a hydrogen dual fueled diesel engine characteristics: An experiment approach, International Journal of Hydrogen Energy (2017), http://dx.doi.org/10.1016/j.ijhydene.2017.04.096

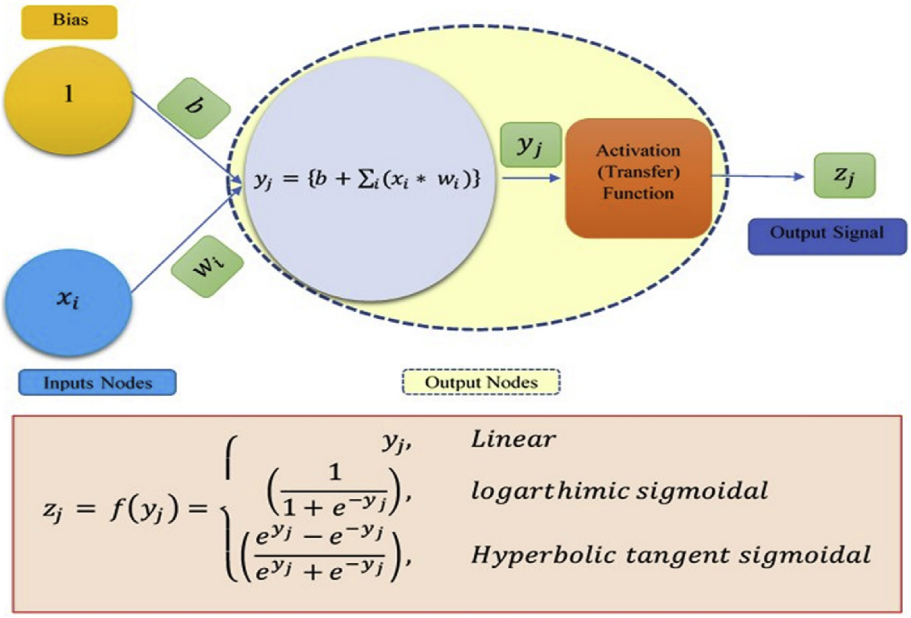


**Fig. 1 – Perceptron configuration with three transfer functions.**

Such process of training perceptron is known as feed-forward backpropagation network. Taking into account of non-linearity in data, additional layer(s) of neurons are included between input and output layer, which leads to the formation of multi-layer perceptron network. Various training algorithm to train the perceptron are Levenberge Marquardt (trainlm), Gradient descent with adaptive learning rate (traingda), Gradient descent with momentum and adaptive learning rate backpropagation (traingdx), Resilient backpropagation (trainrp), Conjugate gradient backpropagation with Fletcher-Reeves updates (traincgf), Scaled conjugate gradient back-propagation (trainscg) and Broyden, Fletcher, Goldfarb, & Shanno (BFGS) quasi-Newton backpropagation (trainbfg). Based upon the nature of the relationship between inputs and targets, the output of perceptron is subjected to either of these transfer functions: Hyperbolic tangent sigmoid (tansig), Log-arithmic sigmoid (logsig) and Linear (purelin). For an efficient model, selection of training algorithm, transfer function and number of neurons in hidden layers plays a decisive role.

## Methods summary

### *Engine test rig*

The current experimentation investigation is conducted on a Kirloskar AV1 engine test rig, specifications of which are detailed in Table 1 and experimental set up is schematically sketched in Fig. 2. Inlet air measurement is done with the aid of U-tube manometer and diesel fuel consumption is measured using a burette and stopwatch. Volumetric flow rate of $H_2$ is controlled with the help of a rotameter and pressure with a pressure regulator valve. $H_2$ being highly inflammable, backfire propagation of flame is arrested using flame arrestor and flash arrestor. $H_2$ is premixed with air in an enrichment chamber attached ahead to the inlet port and mixture is inducted through the inlet valve of the engine. Diesel fuel is injected directly into the cylinder with the help of a mechanical injector; details of fuel injection are presented in Table 2. Thermocouples are installed at various positions of set up to register temperatures. The digital tachometer is employed to record engine speed; a governor maintains the constant engine speed of 1500 rpm. An AC alternator is coupled to the engine to evaluate power generation in terms of kW; heating coils are connected to an alternator to employ load on the engine. All the sensors are coupled to data acquisition card to register the reading digitally. Emission parameters are observed with a Mars multi-gas analyzer, specifications of emission analyzer are tabulated in Table 3.

### *Experimentation*

Cooling water to the engine is turned ON, and a flow rate of 3 l/min is maintained using a rotameter. The engine is made to run on standard diesel fuel. Emission analyzer is warmed for 7 min and ensured that a display of 20.9% for oxygen reading

**Table 1 – Technical specifications of the test rig.**

| Sl. no. | Parameter | Specification |
|---|---|---|
| 1 | Make | Kirloskar |
| 2 | Model | AV1 |
| 3 | Type | Single-cylinder, Four-stroke, Direct Injection, Water-cooled CI Engine |
| 4 | Rated power | 3.7 kW @1500 rpm |
| 5 | Bore & Stroke | 80 × 110 mm |
| 6 | Swept volume | 0.553 l |
| 7 | Governing class | $B_1$ as per IS:10000 |
| 8 | Compression ratio | 16.5:1, Range: 13.51–20 |
| 9 | Dynamometer | Electrical AC Alternator, PF: 0.7 |
| 10 | Orifice diameter | 20 mm |

Please cite this article in press as: Syed J, et al., Artificial Neural Network modeling of a hydrogen dual fueled diesel engine characteristics: An experiment approach, International Journal of Hydrogen Energy (2017), http://dx.doi.org/10.1016/j.ijhydene.2017.04.096

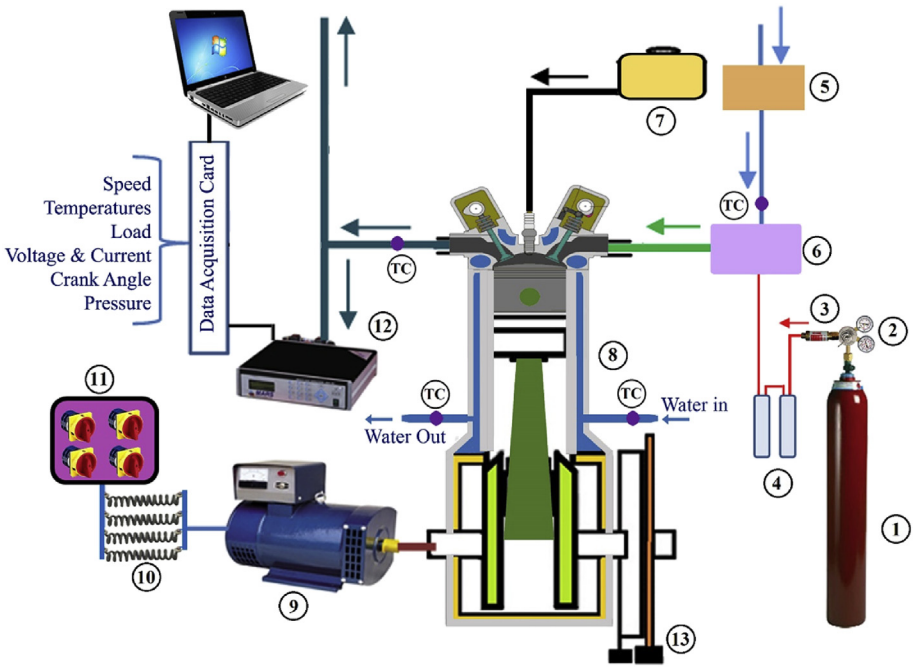


**Fig. 2 – Experimental set up (1. $H_2$ Cylinder, 2. Pressure Regulator, 3. Flash Back Arrestor, 4. Flame Arrestor, 5. Air Tank, 6. Enrichment Unit, 7. Liquid Fuel Tank, 8. IC Engine, 9. AC Dynamometer, 10. Heating Elements, 11. Load Control Panel, 12. Emission Analyser, 13. Crank Angle Sensor, TC. Thermocouple).**

while other parameters show 0% reading. Load on the engine is applied by switching-ON 0.5 kW heating element. The temperature at the outlet of cooling water is monitored, when the constant temperature is attained i.e. steady state condition of operation, time for 20 ml of diesel consumption, generator voltage & current, emission parameters and EGT are registered. The same procedure is repeated for 1, 2 and 3 kW engine load.

The engine is allowed to cool to room temperature; it is ensured that cooling water inlet and outlet temperatures are same. The engine is run on diesel fuel, and $H_2$ (99.9% purity) at a pressure of 1 bar is allowed to flow at 0.5 l/min. Performance and emissions parameters are recorded for all the loads at steady state operating condition. The above process is repeated for 1 and 1.5 l/min $H_2$ flow rate for 1, 2 and 3 kW engine load.

### *Uncertainty analysis*

Experimentation on engine engrosses range of instruments to measure different parameters. Instrument holds certain error in the measurement of the parameter known as fixed error.

**Table 2 – Details of diesel fuel injector.**

| Sl. no. | Parameter | Specification |
|---|---|---|
| 1 | Make | Bosch |
| 2 | Type | Mechanical |
| 3 | Injection pressure | 210 bar |
| 4 | Number of holes | 3 |
| 5 | Nozzle diameter | 0.15 mm |
| 6 | Injection advance | 23° top dead center |

Other factors like environmental conditions also lead to inaccuracy in measurement. Directly measured parameters include all such errors. Hence, total uncertainty in measurable parameters needs to be evaluated. The validity of such measurements is carried out with a degree of ambiguity in measurement. Parameter's measurable total uncertainties, in turn, propagate to computed parameter accuracy. The accuracy of the experimentation depends on all uncertainties involved. Each set of experiments is repeated for three times and mean is considered for evaluating computed parameters or analyzing the results. Estimation of uncertainty in measurable and computed parameters is presented in Tables 4 and 5 respectively. Formulation of uncertainty with a sample calculation is provided in Appendix A. Uncertainty of the experiment when the engine is run on diesel fuel with an $H_2$ flow rate of 1.5 l/min at 3 kW load is stretched amidst 0.5 and 2.1%.

### *Development of ANN model*

Efficacy of the ANN model depends upon the data used to train the model. Hence, significant care must be taken in generating experiment data within acceptable uncertainty limits. The uncertainty tallies presented in Tables 4 and 5 shows the tolerances of the data generated from the current research work. In the current research, load and $H_2$ flow rate are considered as inputs to the network whereas, BTE, BSFC, CO, $NO_x$, HC (hydrocarbon) and EGT as targets. The network architecture showing input, hidden and the output layer is represented in Fig. 3. With a combination of four loads, three $H_2$ flow rate and diesel fuel, 16 data sets are generated from experiment work. Proper utilization of data plays a crucial role

Please cite this article in press as: Syed J, et al., Artificial Neural Network modeling of a hydrogen dual fueled diesel engine characteristics: An experiment approach, International Journal of Hydrogen Energy (2017), http://dx.doi.org/10.1016/j.ijhydene.2017.04.096

**Table 3 – Emission analyzer specifications.**

| Sl. no. | Measured qty. | Measuring range | Accuracy | Resolution | Others |
|---|---|---|---|---|---|
| 1 | CO | 0–10.0 vol% | +/– 0.01 vol% | 0.01 vol% | |
| 2 | HC | 0–1000 ppm | +/– 1 ppm | 1 ppm | |
| 3 | $NO_x$ | 0–2000 ppm | +/– 1 ppm | 1 ppm | |
| 4 | – | – | – | – | Warm up time: 7 min |
| 5 | – | – | – | – | Response time: < 15s |
| 6 | – | – | – | – | PC Interface: Yes, RS 232 |

**Table 4 – Sample estimation of uncertainty (%) in measurable parameters at a 3 kW load for diesel fuel with $H_2$ flow rate of 1.5 l/min.**

| Measured Parameter | Test-1 | Test-2 | Test-3 | Mean=$\overline{X}$ | Variable error with 95% confidence level = 2σ | % $U_{.95} = \frac{2\sigma * 100}{\overline{X}}$ | % Fixed error of Instrument (FEI) | % *Total Uncertainty in measurement(TU)* $= \sqrt{U_{.95}^2 + FEI^2}$ |
|---|---|---|---|---|---|---|---|---|
| HC (ppm) | 7 | 7 | 7 | 7 | 0.000 | 0.000 | 0.5 | 0.50 |
| CO (vol%) | 0.189 | 0.186 | 0.19 | 0.188 | 0.003 | 1.737 | 0.5 | 1.81 |
| $NO_X$ (ppm) | 321 | 320 | 322 | 319 | 2.494 | 0.779 | 1.5 | 1.69 |
| EGT (°C) | 209 | 207 | 209 | 211 | 3.266 | 1.563 | 1 | 1.86 |

in developing a proficient model. Owing to fewer data sets available, the leave-one-out (an extreme version of cross-validation) method is adopted to train the model [13,14]; the network model is developed with all data sets leaving one set for validation of the model. The process is repeated for another 15 times, so that entire data set gets involved in training the network. Though such method of developing the model is very intensive, the performance of the model is noteworthy as all data sets are virtually participated in training the network [15]. Before feeding the network with the data sets, normalization of data between 0.1 and 0.9 [16] need to be computed by using Eq. (1) [9,17,18]. The range of values for experiment data are shown in Table 6. The data is randomized before feeding to train the model.

$$\text{Normalized value} = \left\{ (\textit{Upper Limit} - \textit{Lower limit}) * \left( \frac{\textit{Experiment value} - \textit{Experiment value}_{Min.}}{\textit{Experiment value}_{Max.} - \textit{Experiment value}_{Min.}} \right) + \textit{Lower limit} \right\} \quad (1)$$

Current ANN model is developed on MATLAB platform, a flow chart representing the development process is shown in Fig. 4. Multi-layer perceptron network with one hidden layer is considered for present research work. Counters used for iterations are initialized before training the model, and weights initialization are done randomly. All the 16 models are trained with various training algorithms such as trainlm, traingda, traingdx, trainrp, traincgf, trainscg and trainbfg, whereas combinations of transfer functions (tansig, logsig, purelin) are employed with each algorithm. For every algorithm with a combination of transfer function, number of neurons in the hidden layer is varied from 1 to 25. Statistical benchmark indices such as Root Mean Squared Error (RMSE), Mean Absolute Percentage Error (MAPE), Regression Coefficients (R), Nash– Sutcliffe Efficiency (NSE) and Kling-Gupta Efficiency (KGE) are adopted for adjudging the proficiency of the trained model. The indices are computed using Eqs. (2)–(6). While training ANN model, the minimum gradient of $10^{-7}$ and 10,000 epochs are used as stopping criteria. In the process of attaining the acceptable tolerance for benchmarks, a model with local minima may result; this is prevented by iterating the above process for 100 times. Out of all trained models with various combinations of algorithms and transfer functions, ANN model having global minima is simulated for all 16 input data sets to realize corresponding outputs of the model. De-normalization of simulated results is computed following Eq. (7).

$$\text{RMSE} = \sqrt{\frac{1}{n}\left\{ \sum_{i=1}^{n} (T_i - O_i)^2 \right\}} \quad (2)$$

$$\text{MAPE} = \left\{ \frac{100}{n} \sum_{i=1}^{n} \left| \left( \frac{T_i - O_i}{T_i} \right) \right| \right\}\% \quad (3)$$

Please cite this article in press as: Syed J, et al., Artificial Neural Network modeling of a hydrogen dual fueled diesel engine characteristics: An experiment approach, International Journal of Hydrogen Energy (2017), http://dx.doi.org/10.1016/j.ijhydene.2017.04.096

**Table 5 – Uncertainty (%) in performance parameters and their relevant measurable parameters at a 3 kW load for diesel fuel with $H_2$ flow rate of 1.5 l/min.**

| Parameter | Variable | Uncertainty in measurement or computation |
|---|---|---|
| Voltage | Voltage in V | +/− 2 |
| Current | Current in A | +/− 0.01 |
| Diesel fuel volume measurement (Burette) | Volume in ml | +/− 0.2 |
| Time measurement for diesel fuel consumption | Time in s | +/− 1 s |
| H2 flow measurement (Rotameter) | Flow rate in l/min | +/− 0.015 |
| Brake power | Voltage, Current | +/− 0.827% |
| Mass flow rate of diesel fuel | Volume of diesel fuel, Time | +/− 1.94% |
| Mass flow rate of $H_2$ | Flow rate of $H_2$ | +/− 1% |
| Total fuel consumption | Volume of diesel fuel, Time, Flow rate of $H_2$ | +/− 1.927% |
| BSFC | Brake Power, Total fuel consumption | +/− 2.1% |
| BTE | Brake Power, Volume of diesel fuel, Time, Flow rate of $H_2$ | +/− 0.89% |

$$R = \sqrt{1 - \left\{\frac{\sum_{i=1}^{n}(T_i - O_i)^2}{\sum_{i=1}^{n} O_i^2}\right\}} \quad (4)$$

$$NSE = \left(1 - \frac{MSE}{\sigma_T^2}\right) \quad (5)$$

$$KGE = \left\{1 - \sqrt{\left[(\alpha - 1)^2 + (\beta - 1)^2 + (\gamma - 1)^2\right]}\right\} \quad (6)$$

$$De - Normalized\ value = \left\{sim.value_{ANN} * \left(\frac{Max.\ value_{Exp.} - Min.\ value_{Exp.}}{2}\right) + \left(\frac{Max.\ value_{Exp.} + Min.\ value_{Exp.}}{2}\right)\right\} \quad (7)$$

## Results and discussion

During the experimentation, volumetric flow rate of inlet air and cooling water are maintained constant. While varying the engine load and $H_2$ flow rate, performance characteristic's parameters and emission characteristics are recorded. Based on the performance and emission characteristic's data emanated from the current experimentation, ANN model is developed.

### *Performance characteristics*

#### *Brake thermal efficiency*

Brake Thermal Efficiency is the measure of engine efficiency to convert heat energy of fuel to mechanical energy. In the current experiment set up, the engine is coupled to an AC generator. The output of the generator is measured in terms of voltage (V) and current (I) which intern is used in evaluating the BTE following Eq. (8).

$$\text{Brake Thermal } Efficiency = \left\{\frac{\left(\frac{V*I}{0.7*1000}\right)*100}{(M_D*CV_D) + \left(M_{H_2}*CV_{H_2}\right)}\right\}\% \quad (8)$$

Engine load is varied for a different flow rate of $H_2$ and BTE is plotted against load as depicted in Fig. 5. At a particular load, when the $H_2$ flow rate is increased from 0 to 1.5 l/min, it is noted that diesel fuel consumption decreases. This clearly shows $H_2$ fuel is taking part in the combustion process. The addition of $H_2$ contributes to the increase of in-cylinder peak pressure and temperature, brings positive effect on engine efficiency [19]. From Fig. 5 it is noted that in comparison to diesel fuel, the supply of $H_2$ shows better BTE except at peak load condition. With the induction of $H_2$ at peak engine load condition, abnormal combustion occurs due to shortened ignition duration and ignition delay [20], leading to drop in BTE compared to diesel fuel. Effect of $H_2$ flow rate variation is marginal at low load condition due to a low in-cylinder temperature which is in confirmation of results in the literature [21,22].

#### *Brake specific fuel consumption*

It is a measure of fuel consumption to develop a unit brake power and is evaluated as per Eq. (9). Fig. 6 exemplified variation of BSFC on engine load. $H_2$ has higher diffusivity of 0.63 $cm^2/s$ with air, forms a perfectly homogeneous mixture with air and diesel. $H_2$ dual fueled engine having better combustion process than diesel fuel when substitutes the diesel fuel, BSFC of engine enhances. A similar trend is observed by researchers [21,23,24]. Due to higher combustion temperatures at peak load condition, combustion duration is shortened leading to escape of unburned fuel during exhaust. Moreover, at higher loads with an increase in $H_2$ flow rate, air-$H_2$ fuel ratio decrease causing loss of volumetric efficiency [25]; lead to marginal increase in BSFC compared to 2/3rd load condition which is in lines with the observation of Lilik et al. [26] and Hamdan et al. [27].

$$\text{Brake Specific Fuel } Consumption = \left\{\frac{(M_D + M_{H_2})*3600}{\left(\frac{V*I}{0.7*1000}\right)}\right\} kg/kW - h \quad (9)$$

Please cite this article in press as: Syed J, et al., Artificial Neural Network modeling of a hydrogen dual fueled diesel engine characteristics: An experiment approach, International Journal of Hydrogen Energy (2017), http://dx.doi.org/10.1016/j.ijhydene.2017.04.096

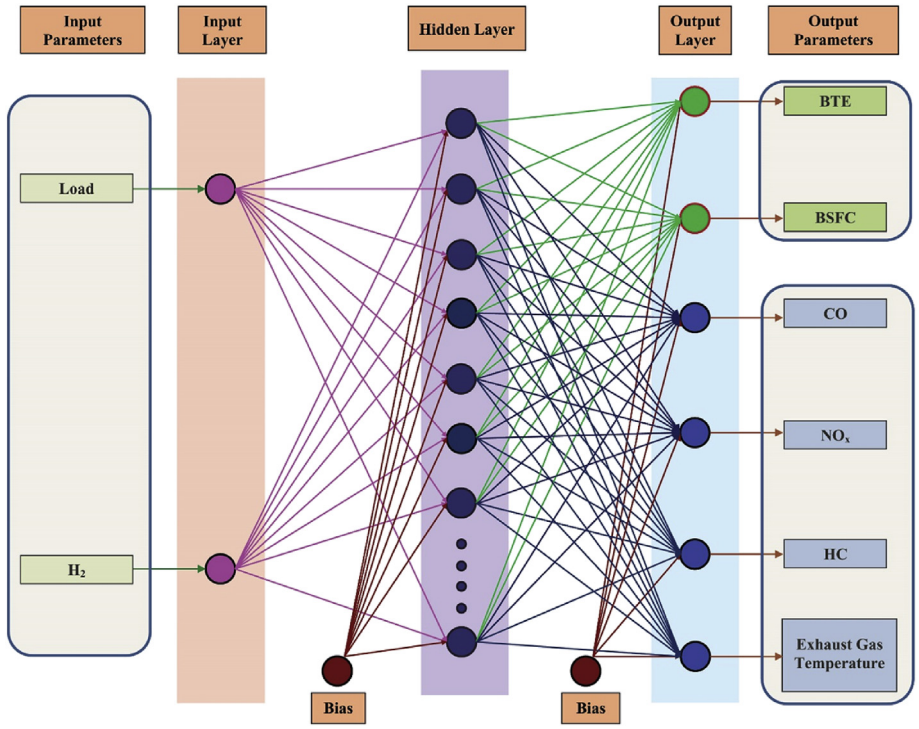


**Fig. 3 – Artificial Neural Network architecture of present research work.**

### *Emission characteristics*

*Carbon monoxide emission*

Carbon monoxide is formed when there is insufficient oxygen during the combustion process. It is colorless, odorless and tasteless with a density slightly less than air. In general, diesel engines are operated under a lean stoichiometry. The principal path of CO formation is shown in Eq. (10) where R is hydrocarbon radical [28].

$$RH \rightarrow R \rightarrow RO_2 \rightarrow RCHO \rightarrow RCO \rightarrow CO \quad (10)$$

CO emission variations for different $H_2$ flow rate are plotted against engine load and are illustrated in Fig. 7. With the increase in engine load, the air-fuel ratio decreases leading to incomplete combustion of fuel resulting increase in CO emissions. This is a normal tendency as registered in the literature [29]. $H_2$ being carbon-free fuel, with an increase in $H_2$ flow rate, CO emissions decreases for all load conditions [30]. The reduction in CO emissions, for diesel dual fueled with an $H_2$ flow rate of 1.5 l/min as compared to neat diesel is 41 and 36% at low load and peak load respectively; this is attributed to higher temperatures at peak load condition.

At 1 kW engine load, EGT is found to be lower for $0.5H_2$ flow rate compared to other flow rate, indicating incomplete combustion which in turn resulting in higher CO emission. With the increase in load to 2 kW, air-fuel ratio drop leading to a further increase in CO emissions. This reveals that the addition of $0.5H_2$ flow rate at 1 and 2 kW load does not show any improvement in CO emissions.

**Table 6 – Range of inputs and targets obtained from experiments.**

| Parameter | Minimum value | Maximum value |
|---|---|---|
| Load (kW) | 0.5 | 3 |
| $H_2$ Flow rate (l/min) | 0 | 1.5 |
| BTE (%) | 11.486 | 31.628 |
| BSFC (kg/kWh) | 0.261 | 0.722 |
| HC (ppm) | 1 | 30 |
| CO (vol%) | 0.048 | 0.296 |
| $NO_X$ (ppm) | 87 | 339 |
| EGT (°C) | 111 | 209 |

*Nitrogen oxide emissions*

Nitrogen Oxide emissions are most adverse emission during combustion process [31]. It is a well-known fact that formation of $NO_x$ mainly depends upon in-cylinder temperatures, oxygen content and resident time. Formation of $NO_x$ (nitric oxide and nitrogen dioxide) is as shown in Eqs. (11)–(14) [32]:

$$O + N_2 \leftrightarrow NO + N \quad (11)$$

$$N + O_2 \leftrightarrow NO + O \quad (12)$$

$$N + OH \leftrightarrow NO + H \quad (13)$$

$$NO + H_2O \leftrightarrow NO_2 + H_2 \quad \text{OR} \quad NO + O_2 \leftrightarrow NO_2 + O \quad (14)$$

Fig. 8 demonstrates the variation of $NO_x$ emission over engine load. Similar to CO emission, with induction of $H_2$ at all loads, $NO_x$ emission is improved compared with baseline diesel fuel, this is attributed to an increase in peak heat release rate with $H_2$ [33]. Statistical analysis of results for $H_2$ flow rate variation from 0 to 1.5 l/min shows 3.5% improvement in $NO_x$ emission at peak load (11%) compared to low load (7.5%)

Please cite this article in press as: Syed J, et al., Artificial Neural Network modeling of a hydrogen dual fueled diesel engine characteristics: An experiment approach, International Journal of Hydrogen Energy (2017), http://dx.doi.org/10.1016/j.ijhydene.2017.04.096

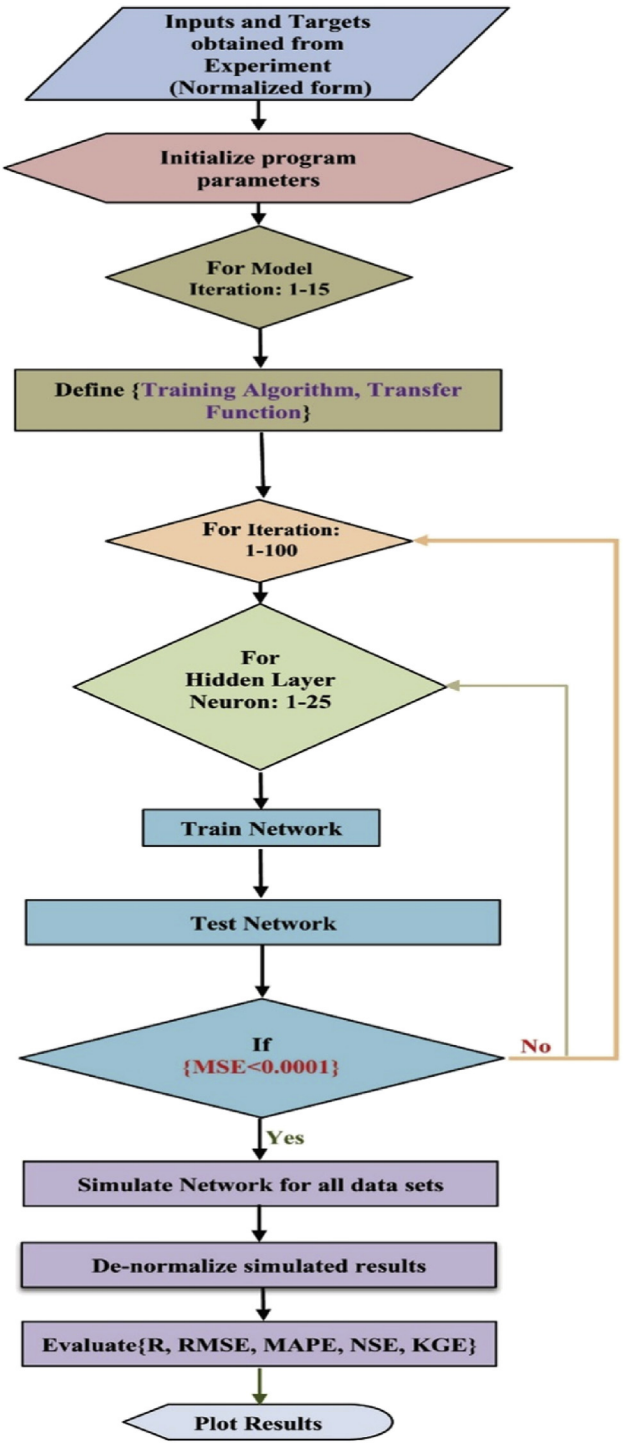


**Fig. 4 – Flow chart of the proposed feed-forward backpropagation neural network model development.**

condition. This is ascribed to higher temperatures at peak load conditions. Correlation between $NO_x$ and EGT is shown in Fig. 9. In-cylinder combustion temperatures increases with increase in engine load, hence $NO_x$ emissions increase with the increase in EGT [34]. Combustion flame temperature is the primary function in the rate of $NO_x$ formation. The results reveal that with induction of $H_2$, $NO_x$ is lowered. Also, at peak load operating condition, the rate of EGT variation is higher than $NO_x$ formation, this is attributed to better combustion phenomena.

*Hydrocarbon emission*

Hydrocarbon emissions are unburnt hydrocarbon resulting from incomplete combustion of fuel due to low combustion temperatures. Such unburnt fuel will be deposited at boundary layers and crevices [35]. Variation of HC emission when the engine load is varied for different $H_2$ flow rate is portrayed in Fig. 10. Due to the high flame speed of $H_2$, the rate of $H_2$ combustion is fast. With the induction of $H_2$ at low loads, owing to lower combustion temperatures inferior combustion phenomena occurs resulting in the escape of unburnt HC. The repercussion of increasing load is a rise in combustion temperatures, resulting lessening of HC emissions. Current results are similar to observations found in the literature [21,22]. At peak engine load, the $H_2$ flow rate of 0.5 l/min show lower HC emission; this is attributed to lean $H_2$ fuel mixture. HC emission decreases with the induction of $H_2$, nevertheless, increases for $1.5H_2$ flow rate. This phenomenon is attributed to the high flame speed of combustion with the high $H_2$ flow rate.

*Exhaust gas temperature*

Variation of exhaust gas temperature with engine load is delineated in Fig. 11. Experimental investigation reveals that maximum rate of pressure rise and peak pressure increases with induction of $H_2$ in a dual fuel engine operation [36]. For all loads, diesel fuel presents low EGT compared to $H_2$ induction [37]. This is imputed to rise in heat release rate when $H_2$ is induced [19,38]. At peak operating load condition, $H_2$ with 1.5 l/min flow rate demonstrations 2.5% increase in EGT compared to baseline diesel fuel.

### *Emission-performance trade-off study*

Depletion of fossil fuel and emissions are the major concerns of the globe [39]. The paradigm is to reconnoiter fuel which possesses better BSFC and least harmful emission characteristics. Literature reveals comprehensive trade-off analysis was evaluated on $NO_x$, HC, soot, and BSFC for the ingenious fuels tested [32,39-41].

In the similar lines, for the present study, $NO_x$, HC, and BSFC trade-off contours are plotted to analyze flow rate of $H_2$ at which performance and emission characteristics are found to be optimum. The trade-off contours for all engine load conditions obtained for different $H_2$ flow rate are shown in Fig. 12. The dash lines indicate the variation of $NO_x$ with HC when the $H_2$ flow rate is varied from 0 to 1.5 l/min. In Fig. 12a when the $H_2$ flow rate is increased from 0 to 0.5 l/min, $NO_x$, HC and BSFC decreases. Further $H_2$ enrichment results in a decrease in BSFC and $NO_x$ but HC increases. It is evident from Fig. 12a that at low engine load, the $H_2$ flow rate of 1 l/min results in low BSFC and HC emission but higher $NO_x$ compared to 1.5 l/min $H_2$ flow rate. Fig. 12b show improvement in performance and emissions with an increase in $H_2$ flow rate from 0 to 1 l/min. Further increase in $H_2$ flow rate results improvement in $NO_x$ and BSFC but HC emissions increase. Hence, in the case of engine running on 1 kW load, the optimum $H_2$ flow rate with better performance and emission

Please cite this article in press as: Syed J, et al., Artificial Neural Network modeling of a hydrogen dual fueled diesel engine characteristics: An experiment approach, International Journal of Hydrogen Energy (2017), http://dx.doi.org/10.1016/j.ijhydene.2017.04.096

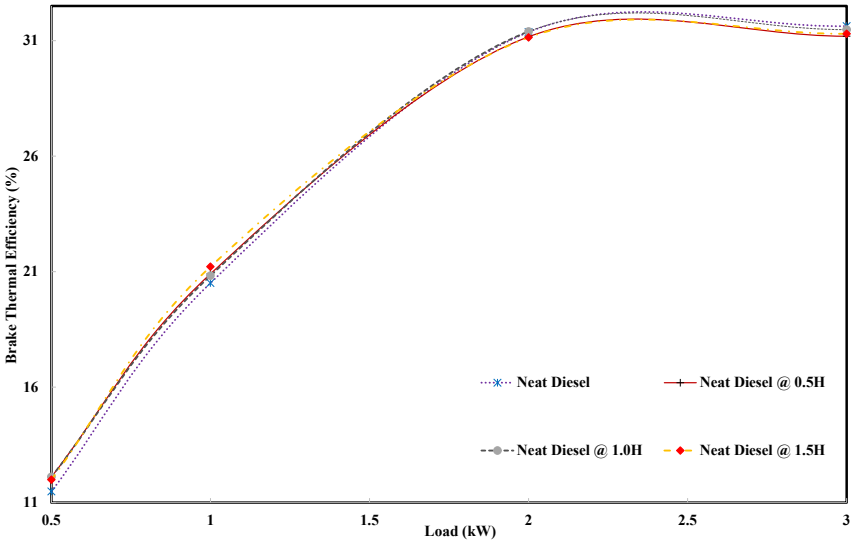


**Fig. 5 – Variation of BTE with load for various fuel combinations.**

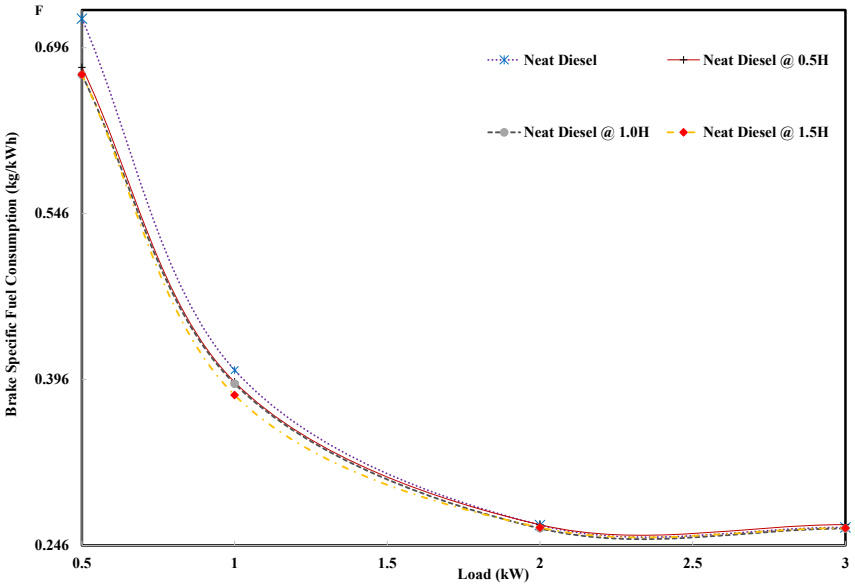


**Fig. 6 – Variation of BSFC with load for various fuel combinations.**

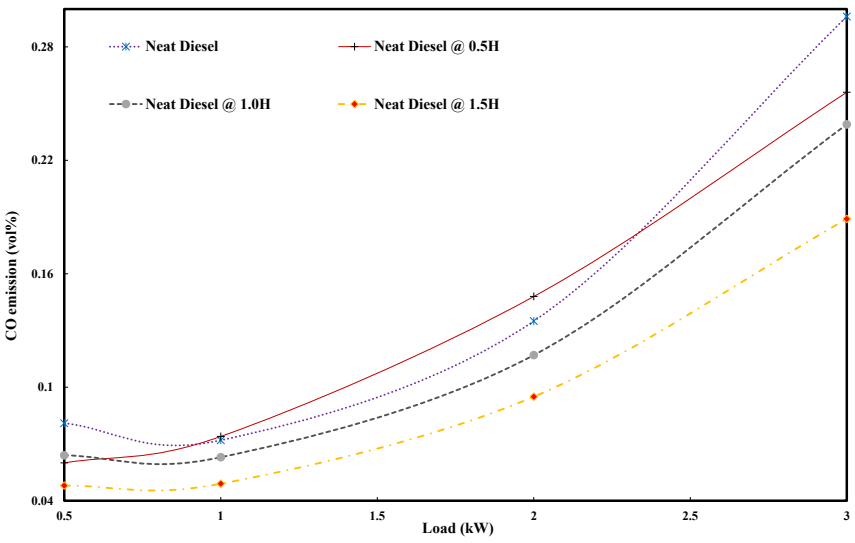


**Fig. 7 – Variation of CO emission with load for various fuel combinations.**

Please cite this article in press as: Syed J, et al., Artificial Neural Network modeling of a hydrogen dual fueled diesel engine characteristics: An experiment approach, International Journal of Hydrogen Energy (2017), http://dx.doi.org/10.1016/j.ijhydene.2017.04.096

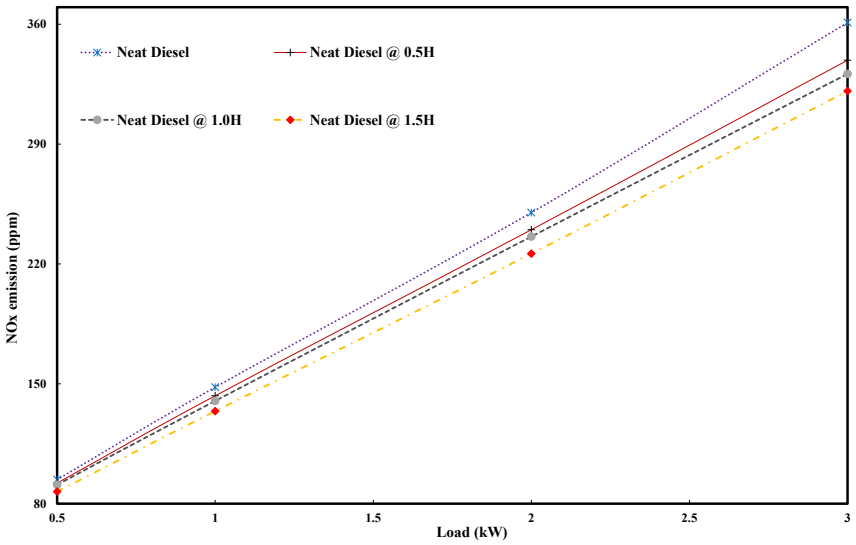


**Fig. 8 – Variation of $NO_x$ emission with load for various fuel combinations.**

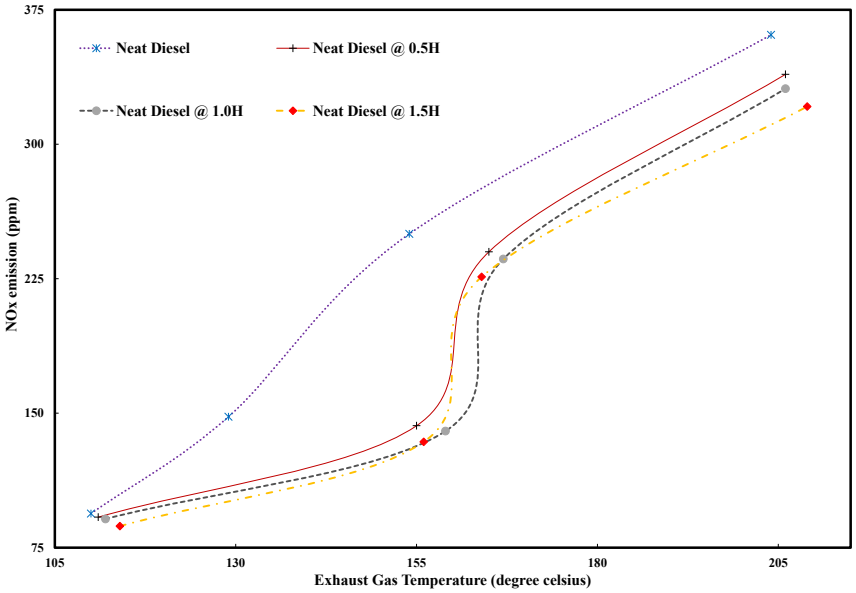


**Fig. 9 – Variation of $NO_x$ emission with EGT for various fuel combinations.**

characteristics is 1 l/min. In the case of 2 kW engine load, increase in $H_2$ flow rate from 0 to 1 l/min, $NO_x$, HC and BSFC decreases. Further increase in $H_2$ flow rate leads to increase in HC emission. From Fig. 12c it is figured out that $H_2$ flow rate of 1 l/min is the optimum to obtain a trade-off between performance and emission characteristics. At peak engine load of 3 kW operating condition (Fig. 12d), $NO_x$, HC, and BSFC decrease when the $H_2$ flow rate is varied from 0 to 1.5 l/min except for 0.5 l/min. At 0.5 l/min flow rate, fuel consumption is high, but HC emissions lowered. The current trade-off results reveal that for peak load engine operating condition, the $H_2$ flow rate of 1.5 l/min is suitable to attain better performance and emission characteristics.

### *ANN predictions*

Credible data generated by varying engine load and the $H_2$ flow rate is fed to the network to develop the competent model. Eight combinations of transfer functions were tested with each training algorithm while varying the number of neurons in the hidden layer. The predictions obtained by feeding all 16 data set inputs are de-normalized to weigh the performance of the model with benchmark indices. The best benchmark indices obtained from 16 model iterations for every training algorithm and transfer function combination are tabulated in Tables B.1–B.7. The Number of neurons in the hidden layers is also depicted in Tables B.1–B.7. Scrutiny of

Please cite this article in press as: Syed J, et al., Artificial Neural Network modeling of a hydrogen dual fueled diesel engine characteristics: An experiment approach, International Journal of Hydrogen Energy (2017), http://dx.doi.org/10.1016/j.ijhydene.2017.04.096

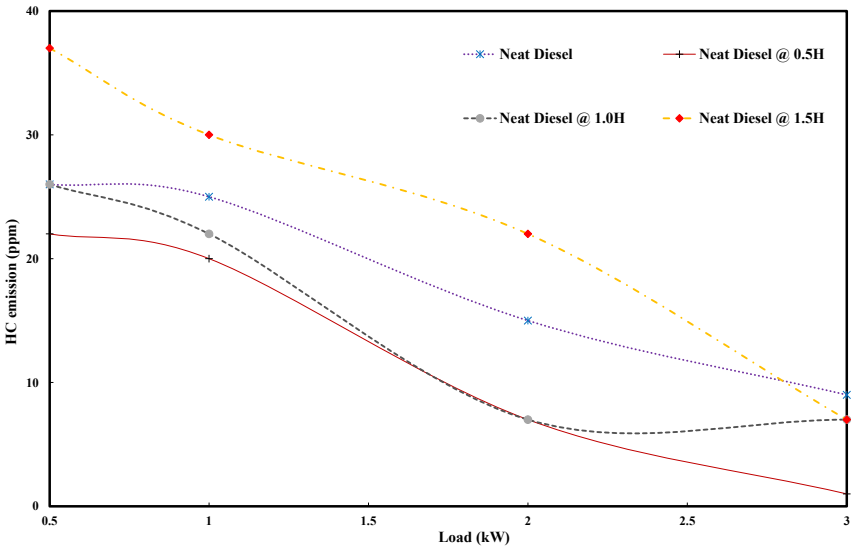


**Fig. 10 – Variation of HC emission with load for various fuel combinations.**

indices obtained for various training algorithms reveals tansig–tansig transfer function combination leads to the best performance of the model. Also, Tables B.1–B.7 infer that predictions obtain with tansig–logsig, logsig–logsig, purelin–logisg and purelin–tansig are not within acceptable tolerances. Out of seven training algorithms tested trainbfg stand out as the best model for the current research work. Trainbfg algorithm is based upon the quasi-Newton method and can train any network as long as its inputs, weights and transfer functions have derivative functions. Back propagation is used to calculate performance function (MSE) with respect to the weights and bias; trainbfg algorithm is robust showing first-rate convergence [42].

Benchmark indices obtained for trainbfg algorithm with tansig–tansig transfer function are portrayed in Table B.7. Predictions of the model for trainbfg algorithm with tansig–tansig transfer function are compared with the current experiment results. Regression plots and predictions of ANN model developed in de-normalized form are presented in Figs. 13–18 for performance parameter BTE & BSFC and emission parameter CO, $NO_x$, HC & EGT. Regression plots represent closeness of predictions to experimental results; higher regression coefficient indices indicate higher prediction accuracy of the model. Apart from regression coefficient, RMSE, MAPE, NSE and KGE are presented in the regression plot to evaluate the proficiency of the model. For an accurate model, the RMSE and MAPE of predictions must be close to zero. A meticulous insight into the regression and experiment-prediction comparison plots, standard benchmark indices demonstrate the efficacy of the developed model. Regression

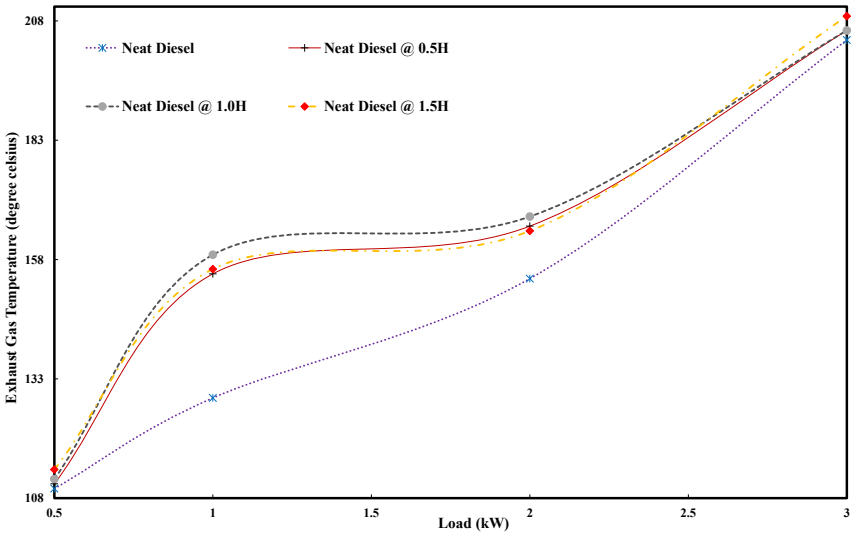


**Fig. 11 – Variation of EGT with load for various fuel combinations.**

Please cite this article in press as: Syed J, et al., Artificial Neural Network modeling of a hydrogen dual fueled diesel engine characteristics: An experiment approach, International Journal of Hydrogen Energy (2017), http://dx.doi.org/10.1016/j.ijhydene.2017.04.096

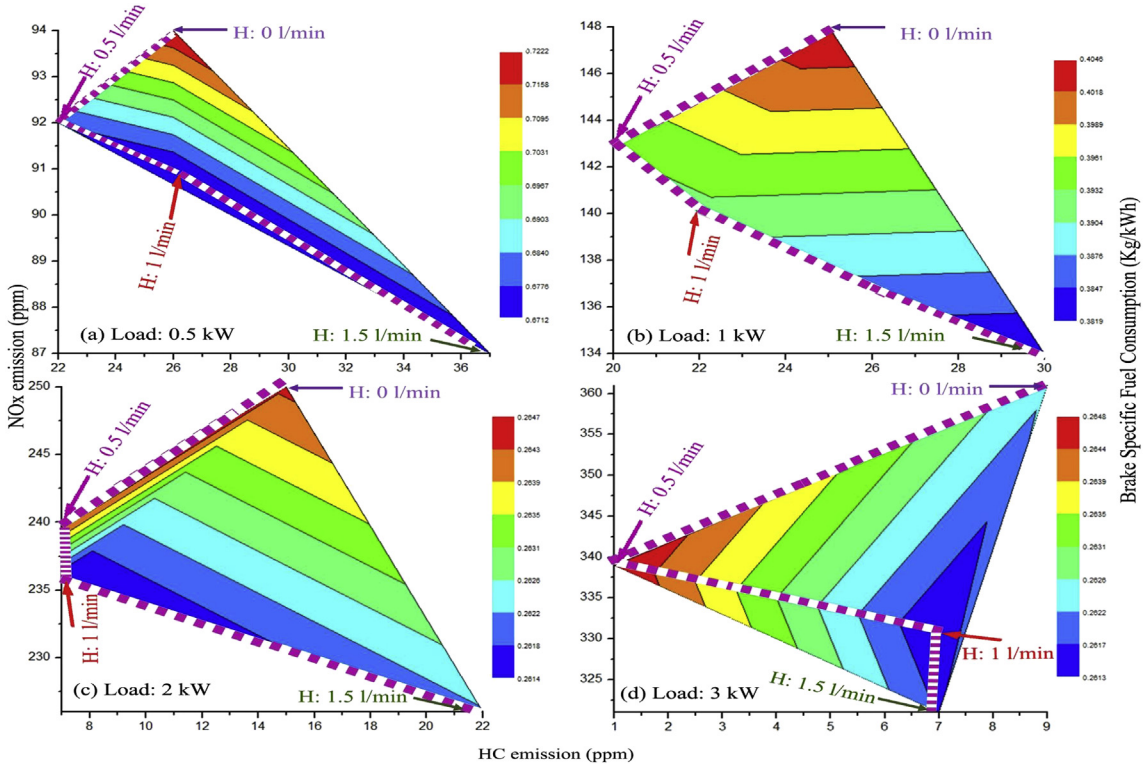


**Fig. 12 – Emission-performance trade-off plots for various fuel combinations at different load conditions.**

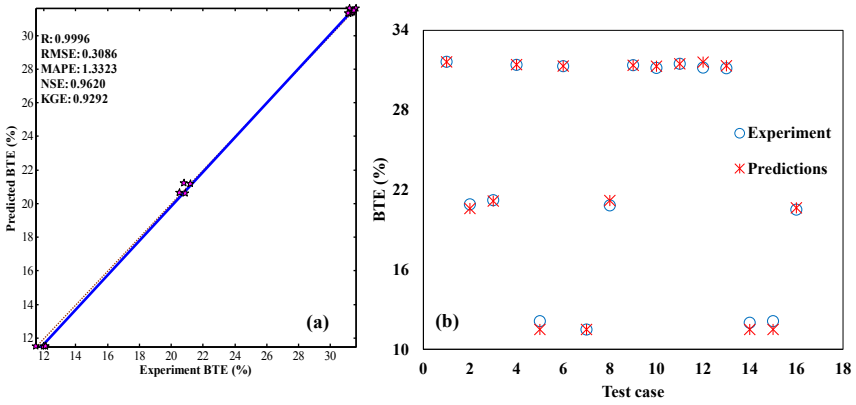


**Fig.13 – (a) Regression plot for BTE and (b) Experiment and predicted BTE comparison for all 16 data sets.**

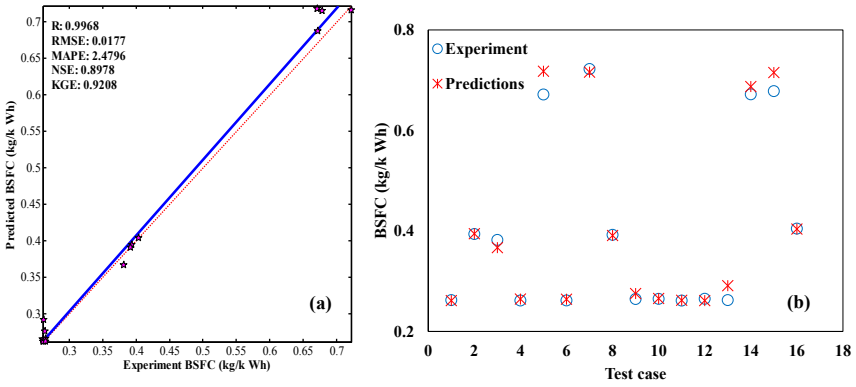


**Fig.14 – (a) Regression plot for BSFC and (b) Experiment and predicted BSFC comparison for all 16 data sets.**

Please cite this article in press as: Syed J, et al., Artificial Neural Network modeling of a hydrogen dual fueled diesel engine characteristics: An experiment approach, International Journal of Hydrogen Energy (2017), http://dx.doi.org/10.1016/j.ijhydene.2017.04.096

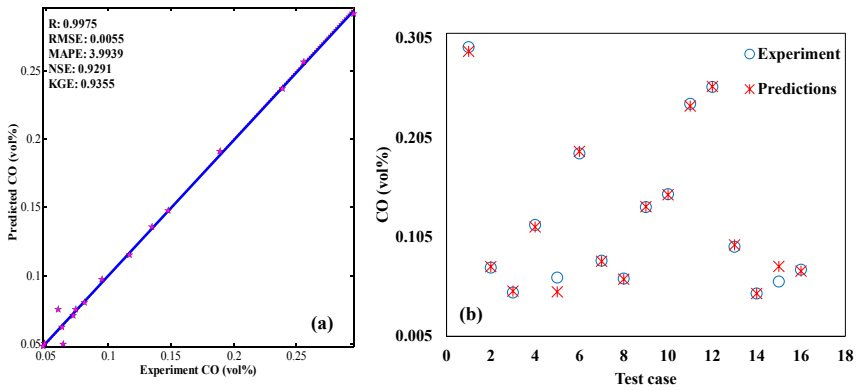


**Fig.15 – (a) Regression plot for CO emission and (b) Experiment and predicted CO emission comparison for all 16 data sets.**

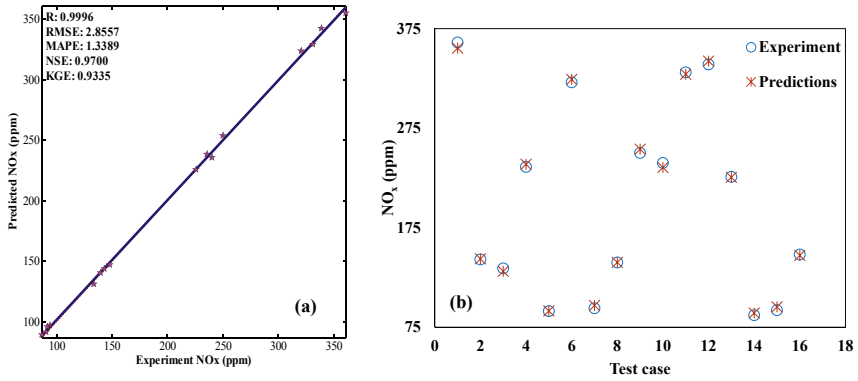


**Fig.16 – (a) Regression plot for $NO_x$ emission and (b) Experiment and predicted $NO_x$ emission comparison for all 16 data sets.**

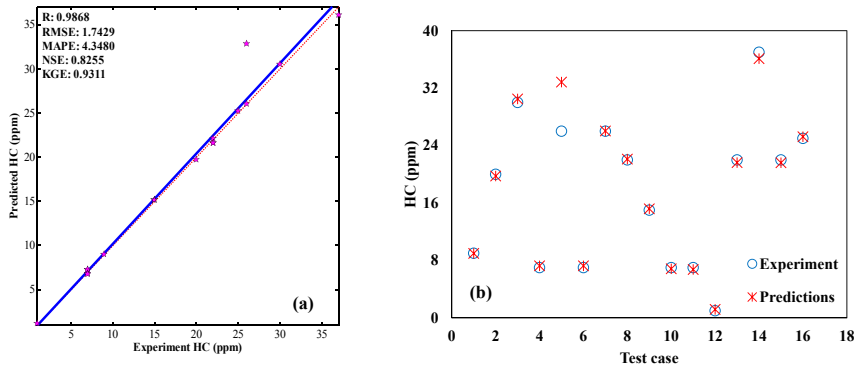


**Fig.17 – (a) Regression plot for HC emission and (b) Experiment and predicted HC emission comparison for all 16 data sets.**

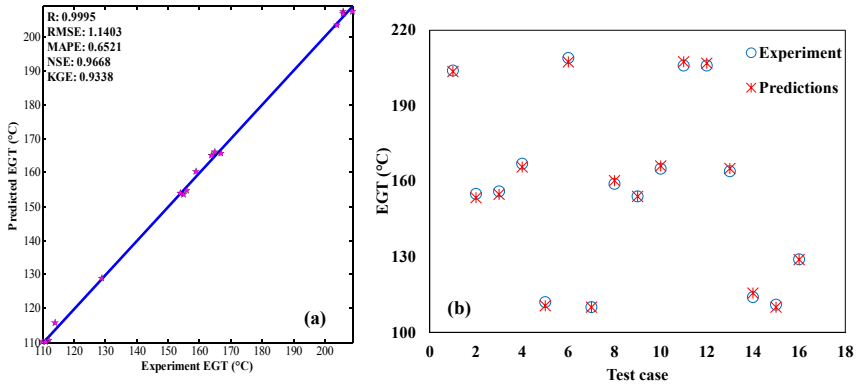


**Fig.18 – (a) Regression plot for EGT and (b) Experiment and predicted EGT comparison for all 16 data sets.**

Please cite this article in press as: Syed J, et al., Artificial Neural Network modeling of a hydrogen dual fueled diesel engine characteristics: An experiment approach, International Journal of Hydrogen Energy (2017), http://dx.doi.org/10.1016/j.ijhydene.2017.04.096

coefficient of BTE, BSFC, CO, $NO_x$, HC, & EGT are 0.9996, 0.9968, 0.9975, 0.9996, 0.9898 & 0.9995 respectively, whereas NSE stretched between 0.8255 and 0.97.

## Conclusions

With the aim to develop pragmatic ANN model to efficiently predict performance and emission characteristics of $H_2$ dual fueled diesel engine, the experiment is conducted by varying engine load and $H_2$ flow rate. Uncertainty analysis is evaluated to ascertain the error in the outcomes of the experiment. The experiment show, the $H_2$ flow rate has a significant role on performance and emissions characteristics. ANN model with trainbfg algorithm, eight neurons in hidden layer for tansig–tansig transfer function is developed to prediction performance, and emission characteristics of $H_2$ dual fueled diesel engine. The range of RMSE, MAPE, and KGE obtained for predicted parameters are 0.0055–2.8557, 0.521–4.348% and 0.9208–0.9338 respectively. In the view of benchmark indices obtained with the ANN model developed, it is implicit to mention that ANN predictions are precisely matching with the experiment outcomes.

## Acknowledgements

The authors would like to express their gratitude to King Khalid University, Saudi Arabia for providing administrative and technical support.

## Appendix A. Uncertainty in computed parameters.

The following formulations adopted to estimate the uncertainties of performance parameters:

### A.1. Brake power (BP)

$$BP = (VI/700)kW$$

where V: Voltage in V and I: Current in A.

$$\frac{\partial BP}{\partial V} = \frac{I}{700}$$

$$\frac{\partial BP}{\partial I} = \frac{V}{700}$$

$$Uncertainity\ in\ BP, i.e\ \Delta BP = \left[\sqrt{\left[\frac{I}{700}*\Delta V\right]^2 + \left[\frac{V}{700}*\Delta I\right]^2}\right]kW$$

$$\Delta BP(\%) = \left(\frac{\Delta BP*100}{BP}\right)\%$$

### A.2. Mass flow rate of Diesel fuel (MFDF) consumption)

$$MFDF = (Vol*10^{-6}*D/T)kg/s$$

where Vol: Volume of diesel fuel in burette in mL, D: Density of diesel fuel in $kg/m^3$ and T is time in s.

$$\frac{\partial MFLF}{\partial Vol} = \frac{D*10^{-6}}{T}$$

$$\frac{\partial MFLF}{\partial T} = (-1)\frac{Vol*D*10^{-6}}{T^2}$$

$$Uncertainity\ in\ MFDF,\ i.e\ \Delta MFDF = \left[\sqrt{\left[\frac{D*10^{-6}}{T}*\Delta Vol\right]^2 + \left[(-1)\frac{Vol*D*10^{-6}}{T^2}*\Delta T\right]^2}\right]kg/s$$

$$\Delta MFDF\ (\%) = \left[\frac{\Delta MFDF*100}{MFDF}\right]\%$$

### A.3. Mass flow rate of $H_2$ (MFH) consumption

$$MFH = (FRH*D_H/60000)kg/s$$

where FRH: Flow rate of $H_2$ in l/min and $D_H$: Density of $H_2$ in $kg/m^3$.

$$\frac{\partial MFH}{\partial FRH} = \frac{D_H}{60000}$$

$$Uncertainity\ in\ MFH,\ i.e\ \Delta MFH = \left[\sqrt{\left[\frac{D_H}{60000}*\Delta FRH\right]^2}\right]kg/s$$

$$\Delta MFH\ (\%) = \left[\frac{\Delta MFH*100}{MFH}\right]\%$$

### A.4. Total fuel consumption (TFC)

$$TFC = 3600(MFDF + MFH)kg/h$$

Please cite this article in press as: Syed J, et al., Artificial Neural Network modeling of a hydrogen dual fueled diesel engine characteristics: An experiment approach, International Journal of Hydrogen Energy (2017), http://dx.doi.org/10.1016/j.ijhydene.2017.04.096

$$\text{Uncertainity in TFC, i.e } \Delta TFC = \left[\sqrt{[3600{*}\Delta MFDF]^2 + [3600{*}\Delta MFH]^2}\right] kg/h$$

$$\Delta TFC\ (\%) = \left[\frac{\Delta TFC{*}100}{TFC}\right]\%$$

### A.5. Brake specific fuel consumption (BSFC)

$$BSFC = (TFC/BP) kg/kWh$$

$$\frac{\partial BSFC}{\partial TFC} = \frac{1}{BP}$$

$$\frac{\partial BSFC}{\partial BP} = (-1)\frac{TFC}{BP^2}$$

$$\text{Uncertainity in BSFC, i.e } \Delta BSFC = \left[\sqrt{\left[\frac{1}{BP}{*}\Delta TFC\right]^2 + \left[(-1)\frac{TFC}{BP^2}{*}\Delta BP\right]^2}\right] kg/kWh$$

$$\text{Uncertainity in BTE, i.e } \Delta BTE = \left[\sqrt{\left[\frac{100}{\gamma}{*}\Delta BP\right]^2 + \left[(-1)\frac{100{*}BP}{\gamma^2}\Delta\gamma\right]^2}\right]\%$$

$$\Delta BSFC\ (\%) = \left[\frac{\Delta BSFC{*}100}{BSFC}\right]\%$$

### A.6. Brake thermal efficiency (BTE)

$$BTE = \{BP{*}100/(MFDF{*}CV_D + MFH{*}CV_H)\}\%$$

where $CV_D$: Lower Calorific value of diesel fuel and $CV_H$: Lower Calorific value of $H_2$.

Let, $\alpha = (MFDF{*}CV_D)$, $\beta = (MFH{*}CV_H)$ and $\gamma = \alpha + \beta$

$$\frac{\partial \alpha}{\partial MFLF} = CV_D$$

$$\frac{\partial \beta}{\partial MFH} = CV_H$$

$$\text{Uncertainity in } \gamma,\ i.e\ \Delta\gamma = \sqrt{[CV_D{*}\Delta MFDF]^2 + [CV_H{*}\Delta MFH]^2}$$

$$\frac{\partial BTE}{\partial BP} = \frac{100}{\gamma}$$

$$\frac{\partial BTE}{\partial \gamma} = (-1)\frac{100 * BP}{\gamma^2}$$

### A.7. Sample evaluation of BP, BSFC and BTE for diesel with 1.5 l/min flow rate of $H_2$ at 3 kW engine load condition

Voltage: 243 ± 2 V.
Current: 11.31 ± 0.01 A.
Diesel fuel in burette: 20 ± 0.2 ml.
Time for diesel fuel consumption: 60 ± 1 s.
$H_2$ flow rate: 1.5 ± 0.015 l/min.
Density of diesel fuel (D): 850 kg/m$^3$
Lower Calorific value of diesel fuel ($CV_D$): 43,400 kJ/kg.
Density of $H_2$ ($D_H$): 0.082 kg/m$^3$
Lower Calorific value of $H_2$ ($CV_H$): 121,000 kJ/kg.

Please cite this article in press as: Syed J, et al., Artificial Neural Network modeling of a hydrogen dual fueled diesel engine characteristics: An experiment approach, International Journal of Hydrogen Energy (2017), http://dx.doi.org/10.1016/j.ijhydene.2017.04.096

A.7.1. Brake power (BP)

$$BP = (VI/700) = 3.926\ kW$$

$$\frac{\partial BP}{\partial V} = \frac{I}{700} = 0.016$$

$$\frac{\partial BP}{\partial I} = \frac{V}{700} = 0.347$$

$$\text{Uncertainty in BP, i.e } \Delta BP = \left(\sqrt{\left[\frac{I}{700}*\Delta V\right]^2 + \left[\frac{V}{700}*\Delta I\right]^2}\right) = 0.033\ kW$$

$$\Delta BP\ (\%) = \left(\frac{\Delta BP*100}{BP}\right)\% = \pm 0.827\%$$

A.7.2. Mass flow rate of diesel fuel (MFDF) consumption

$$MFDF = (Vol*10^{-6}*D/T) = 2.833*10^{-4} kg/s$$

$$\frac{\partial MFDF}{\partial Vol} = \frac{D*10^{-6}}{T} = 14.166*10^{-6}$$

$$\frac{\partial MFDF}{\partial T} = (-1)\frac{Vol*D*10^{-6}}{T^2} = -4.722*10^{-6}$$

Uncertainty in MFDF i.e

$$\Delta MFDF = \left[\sqrt{\left[\frac{D*10^{-6}}{T}*\Delta Vol\right]^2 + \left[(-1)\frac{Vol*D*10^{-6}}{T^2}*\Delta T\right]^2}\right] = \pm 5.506*10^{-6}\ kg/s$$

$$\Delta MFDF\ (\%) = \left[\frac{\Delta MFDF*100}{MFDF}\right]\% = \pm 1.94\%$$

A.7.3. Mass flow rate of $H_2$ (MFH) consumption

$$MFH = (FRH*D_H/60000) = 2.05*10^{-6 kg/s}$$

$$\frac{\partial MFH}{\partial FRH} = \frac{D_H}{60000} = 1.366*10^{-6}$$

$$\text{Uncertainty in MFH i.e } \Delta MFH = \left[\sqrt{\left[\frac{D_H}{60000}*\Delta FRH\right]^2}\right] = \pm 2.05*10^{-8}\ kg/s$$

$$\Delta MFH(\%) = \left[\frac{\Delta MFH*100}{MFH}\right]\ \% = \pm 1\%$$

A.7.4. Total fuel consumption (TFC)

$$TFC = 3600(MFDF + MFH) = 1.0273\ kg/h$$

$$\text{Uncertainty in TFC i.e } \Delta TFC = \left[\sqrt{[3600*\Delta MFDF]^2 + [3600*\Delta MFH]^2}\right] = 0.0198\ kg/h$$

$$\Delta TFC(\%) = \left[\frac{\Delta TFC*100}{TFC}\right]\% = \pm 1.927\%$$

A.7.5. Brake Specific fuel consumption (BSFC)

$$BSFC = (TFC/BP) = 0.2616\ kg/kWh$$

$$\text{Uncertainty in BSFC i.e } \Delta BSFC = \left[\sqrt{\left[\frac{1}{BP}*\Delta TFC\right]^2 + \left[(-1)\frac{TFC}{BP^2}*\Delta BP\right]^2}\right] = 5.5*10^{-3} kg/kWh$$

$$\Delta BSFC\ (\%) = \left[\frac{\Delta BSFC*100}{BSFC}\right]\% = \pm 2.1\%$$

A.7.6. Brake thermal efficiency (BTE)

$$BTE = \{BP*100/(MFDF*CV_D + MFH*CV_H)\} = 31.29\%$$

Let, $\alpha = (MFDF*CV_D) = 12.295$

$$\beta = (MFH*CV_H) = 0.248$$

$$\gamma = \alpha + \beta = 12.543$$

$$\frac{\partial \alpha}{\partial MFLF} = CV_D = 43400$$

$$\frac{\partial \beta}{\partial CVH} = MFH = 2.05^{*}10^{-6}$$

$$\Delta\gamma = \sqrt{[CV_D*\Delta MFDF]^2 + [MFH*\Delta CV_H]^2} = 0.344$$

$$\frac{\partial BTE}{\partial BP} = \frac{100}{\gamma} = 7.97$$

$$\frac{\partial BTE}{\partial \gamma} = (-1)\frac{100*BP}{\gamma^2} = -2.495$$

$$\text{Uncertainty in BTE i.e } \Delta BTE = \left[\sqrt{\left[\frac{100}{\gamma}*\Delta BP\right]^2 + \left[(-1)\frac{100*BP}{\gamma^2}\Delta\gamma\right]^2}\right]\% = \pm 0.89\%$$

Please cite this article in press as: Syed J, et al., Artificial Neural Network modeling of a hydrogen dual fueled diesel engine characteristics: An experiment approach, International Journal of Hydrogen Energy (2017), http://dx.doi.org/10.1016/j.ijhydene.2017.04.096

## Appendix B

**Table B.1 – Benchmark indices in de-normalized form for six output parameter predictions for trainlm with different transfer function combinations.**

| Parameter | Benchmark indices | Transfer function combination | | | | | | | |
|---|---|---|---|---|---|---|---|---|---|
| | | tansig–tansig | logsig–tansig | tansig–logsig | logsig–logsig | logsig–purelin | tansig–purelin | purelin–logsig | purelin–tansig |
| Number of neurons in hidden layer | | 6 | 8 | 7 | 5 | 12 | 7 | 6 | 13 |
| BTE | R | 0.9999 | 0.9994 | 0.9208 | 0.9207 | 0.9995 | 0.9997 | 0.9205 | 0.9997 |
| | RMSE | 0.1433 | 0.3348 | 4.8304 | 4.8317 | 0.2861 | 0.1940 | 4.8327 | 0.2687 |
| | MAPE | 0.5728 | 1.2372 | 11.0837 | 11.1934 | 0.5292 | 0.8314 | 11.2989 | 0.9906 |
| | NSE | 0.9823 | 0.9587 | 0.4045 | 0.4044 | 0.9647 | 0.9761 | 0.4043 | 0.9669 |
| | KGE | 0.9335 | 0.9314 | 0.5869 | 0.5920 | 0.9330 | 0.9335 | 0.5938 | 0.9316 |
| BSFC | R | 0.9996 | 0.9961 | 0.9497 | 0.9502 | 0.9995 | 0.9990 | 0.9504 | 0.9983 |
| | RMSE | 0.0054 | 0.0199 | 0.1692 | 0.1692 | 0.0060 | 0.0077 | 0.1696 | 0.0127 |
| | MAPE | 0.5687 | 1.2821 | 9.8319 | 9.8705 | 0.9786 | 1.6043 | 5.2404 | 1.3374 |
| | NSE | 0.9688 | 0.8851 | 0.0224 | 0.0224 | 0.9653 | 0.9553 | 0.0205 | 0.9267 |
| | KGE | 0.9333 | 0.9078 | 0.3824 | 0.3805 | 0.9329 | 0.9343 | 0.3603 | 0.9241 |
| CO | R | 0.9960 | 0.9981 | 0.8993 | 0.9105 | 0.9952 | 0.9964 | 0.9045 | 0.9744 |
| | RMSE | 0.0077 | 0.0049 | 0.0812 | 0.0812 | 0.0077 | 0.0066 | 0.0813 | 0.0178 |
| | MAPE | 5.6009 | 4.8058 | 9.5870 | 9.8653 | 3.9826 | 4.2493 | 10.4822 | 10.5732 |
| | NSE | 0.9003 | 0.9368 | 0.0482 | 0.0485 | 0.9002 | 0.9149 | 0.0498 | 0.7705 |
| | KGE | 0.9221 | 0.9329 | 0.2523 | 0.2498 | 0.9370 | 0.9358 | 0.2460 | 0.9557 |
| $NO_x$ | R | 0.9987 | 0.9986 | 0.8964 | 0.8775 | 0.9996 | 0.999599 | 0.874012 | 0.993186 |
| | RMSE | 5.3301 | 5.6770 | 8.4548 | 8.5838 | 2.6758 | 2.694544 | 8.49647 | 11.1489 |
| | MAPE | 1.0916 | 3.0658 | 5.6847 | 5.8031 | 0.6647 | 1.449713 | 5.09346 | 6.931407 |
| | NSE | 0.9439 | 0.9403 | 0.1745 | 0.1731 | 0.9718 | 0.971647 | 0.174027 | 0.882687 |
| | KGE | 0.9305 | 0.9291 | 0.4354 | 0.4248 | 0.9335 | 0.933741 | 0.440974 | 0.937738 |
| HC | R | 0.9760 | 0.9873 | 0.8680 | 0.8381 | 0.9866 | 0.969848 | 0.705428 | 0.901854 |
| | RMSE | 2.2460 | 1.7580 | 7.9687 | 8.0216 | 1.7383 | 2.640773 | 8.352417 | 4.377442 |
| | MAPE | 8.4128 | 3.0680 | 11.9990 | 11.0658 | 3.9887 | 5.366445 | 12.5613 | 12.66872 |
| | NSE | 0.7751 | 0.8239 | 0.2020 | 0.1967 | 0.8259 | 0.735545 | 0.163565 | 0.56163 |
| | KGE | 0.9499 | 0.9010 | 0.4156 | 0.4202 | 0.9318 | 0.884639 | 0.389859 | 0.94064 |
| EGT | R | 0.9987 | 0.9997 | 0.8466 | 0.8517 | 0.9937 | 0.997536 | 0.843879 | 0.933804 |
| | RMSE | 1.7665 | 0.8894 | 5.1623 | 5.1608 | 3.9541 | 2.472738 | 5.21237 | 8.34709 |
| | MAPE | 0.8143 | 0.3049 | 8.8447 | 8.8316 | 0.9972 | 1.323201 | 9.17761 | 7.135711 |
| | NSE | 0.9486 | 0.9741 | 0.2683 | 0.2684 | 0.8850 | 0.928099 | 0.266892 | 0.64098 |
| | KGE | 0.9346 | 0.9336 | 0.5559 | 0.5476 | 0.9391 | 0.935743 | 0.553524 | 0.914654 |

Please cite this article in press as: Syed J, et al., Artificial Neural Network modeling of a hydrogen dual fueled diesel engine characteristics: An experiment approach, International Journal of Hydrogen Energy (2017), http://dx.doi.org/10.1016/j.ijhydene.2017.04.096

**Table B.2 – Benchmark indices in de-normalized form for six output parameter predictions for traingda with different transfer function combinations.**

| Parameter | Benchmark indices | Transfer function combination | | | | | | | |
|---|---|---|---|---|---|---|---|---|---|
| | | tansig–tansig | logsig–tansig | tansig–logsig | logsig–logsig | logsig–purelin | tansig–purelin | purelin–logsig | purelin–tansig |
| Number of neurons in hidden layer | | 13 | 20 | 12 | 14 | 14 | 13 | 10 | 5 |
| BTE | R | 0.9997 | 0.9994 | 0.9211 | 0.9214 | 0.9973 | 0.9843 | 0.9207 | 0.9997 |
| | RMSE | 0.2321 | 0.3268 | 4.8353 | 4.8335 | 0.6382 | 1.5099 | 4.8336 | 0.2717 |
| | MAPE | 0.8832 | 1.1215 | 11.4342 | 11.3358 | 1.8478 | 3.9675 | 11.3484 | 0.9797 |
| | NSE | 0.9714 | 0.9597 | 0.4039 | 0.4042 | 0.9213 | 0.8139 | 0.4041 | 0.9665 |
| | KGE | 0.9319 | 0.9330 | 0.5951 | 0.5937 | 0.9295 | 0.9168 | 0.5972 | 0.9322 |
| BSFC | R | 0.9985 | 0.9994 | 0.9490 | 0.9510 | 0.9777 | 0.9748 | 0.9495 | 0.9985 |
| | RMSE | 0.0094 | 0.0073 | 0.1694 | 0.1693 | 0.0370 | 0.0412 | 0.1705 | 0.0095 |
| | MAPE | 1.1567 | 0.9576 | 10.2107 | 10.1633 | 2.8830 | 3.6777 | 11.1808 | 1.2709 |
| | NSE | 0.9459 | 0.9576 | 0.0216 | 0.0220 | 0.7864 | 0.7618 | 0.0150 | 0.9449 |
| | KGE | 0.9348 | 0.9315 | 0.3868 | 0.3930 | 0.9272 | 0.8950 | 0.4356 | 0.9347 |
| CO | R | 0.9841 | 0.9980 | 0.8156 | 0.8783 | 0.9972 | 0.9972 | 0.9450 | 0.9826 |
| | RMSE | 0.0150 | 0.0052 | 0.0824 | 0.0820 | 0.0058 | 0.0058 | 0.0858 | 0.0146 |
| | MAPE | 6.5026 | 4.3892 | 10.6964 | 10.6336 | 4.2771 | 3.9572 | 10.8277 | 9.5255 |
| | NSE | 0.8062 | 0.9332 | 0.8642 | 0.8588 | 0.9251 | 0.9247 | 0.9088 | 0.8112 |
| | KGE | 0.9066 | 0.9342 | 0.2088 | 0.2926 | 0.9363 | 0.9363 | 0.2678 | 0.9488 |
| $NO_x$ | R | 0.9983 | 0.9990 | 0.8670 | 0.8554 | 0.9983 | 0.998946 | 0.877132 | 0.992899 |
| | RMSE | 6.0412 | 4.4215 | 8.5129 | 9.6196 | 5.7611 | 4.472348 | 9.55839 | 11.43842 |
| | MAPE | 2.1754 | 2.6932 | 5.1392 | 5.6396 | 3.1816 | 1.188923 | 5.25008 | 6.970433 |
| | NSE | 0.9364 | 0.9535 | 0.1739 | 0.1622 | 0.9394 | 0.95294 | 0.162853 | 0.87964 |
| | KGE | 0.9328 | 0.9324 | 0.4281 | 0.5101 | 0.9324 | 0.934054 | 0.503289 | 0.938917 |
| HC | R | 0.9757 | 0.9956 | 0.8273 | 0.8911 | 0.9984 | 0.996498 | 0.625866 | 0.885949 |
| | RMSE | 2.8942 | 0.9832 | 8.1073 | 8.8520 | 0.5663 | 0.875944 | 8.547352 | 5.270918 |
| | MAPE | 9.1316 | 10.5804 | 9.1736 | 9.3127 | 8.0970 | 7.542759 | 9.9783 | 8.61457 |
| | NSE | 0.7102 | 0.9015 | 0.1881 | 0.1135 | 0.9433 | 0.91228 | 0.144044 | 0.472155 |
| | KGE | 0.8351 | 0.9315 | 0.4351 | 0.4742 | 0.9347 | 0.93031 | 0.392787 | 0.794136 |
| EGT | R | 0.9992 | 0.9790 | 0.8451 | 0.8425 | 0.9988 | 0.996497 | 0.843736 | 0.930363 |
| | RMSE | 1.5621 | 7.1063 | 5.1883 | 5.1843 | 2.0058 | 3.173086 | 5.21055 | 9.28005 |
| | MAPE | 0.6487 | 1.9526 | 9.9983 | 9.0313 | 0.8990 | 1.26173 | 9.19059 | 6.640392 |
| | NSE | 0.9546 | 0.7934 | 0.2676 | 0.2677 | 0.9417 | 0.907735 | 0.266945 | 0.613852 |
| | KGE | 0.9337 | 0.9535 | 0.5506 | 0.9127 | 0.9338 | 0.929299 | 0.555802 | 0.941575 |

Please cite this article in press as: Syed J, et al., Artificial Neural Network modeling of a hydrogen dual fueled diesel engine characteristics: An experiment approach, International Journal of Hydrogen Energy (2017), http://dx.doi.org/10.1016/j.ijhydene.2017.04.096

**Table B.3 – Benchmark indices in de-normalized form for six output parameter predictions for traingdx with different transfer function combinations.**

| Parameter | Benchmark indices | Transfer function combination | | | | | | | |
|---|---|---|---|---|---|---|---|---|---|
| | | tansig–tansig | logsig–tansig | tansig–logsig | logsig–logsig | logsig–purelin | tansig–purelin | purelin–logsig | purelin–tansig |
| Number of neurons in hidden layer | | 8 | 7 | 10 | 14 | 9 | 6 | 5 | 10 |
| BTE | R | 0.9851 | 0.9995 | 0.9229 | 0.9207 | 0.9995 | 0.9998 | 0.9211 | 0.9997 |
| | RMSE | 1.4545 | 0.2798 | 4.8373 | 4.8343 | 0.2504 | 0.1885 | 4.8356 | 0.3396 |
| | MAPE | 2.6178 | 1.0696 | 7.4425 | 7.3983 | 0.7865 | 0.7519 | 7.4780 | 1.4516 |
| | NSE | 0.8207 | 0.9655 | 0.4037 | 0.4041 | 0.9691 | 0.9768 | 0.4039 | 0.9581 |
| | KGE | 0.9466 | 0.9337 | 0.5938 | 0.5974 | 0.9338 | 0.9332 | 0.6015 | 0.9251 |
| BSFC | R | 0.9995 | 0.9972 | 0.9493 | 0.9519 | 0.9994 | 0.9983 | 0.9490 | 0.9979 |
| | RMSE | 0.0057 | 0.0145 | 0.1695 | 0.1693 | 0.0059 | 0.0103 | 0.1695 | 0.0199 |
| | MAPE | 1.0351 | 1.3062 | 5.4088 | 5.0995 | 1.5058 | 1.4030 | 5.3761 | 1.7137 |
| | NSE | 0.9672 | 0.9160 | 0.0209 | 0.0218 | 0.9659 | 0.9403 | 0.0211 | 0.8850 |
| | KGE | 0.9336 | 0.9264 | 0.3576 | 0.3810 | 0.9338 | 0.9334 | 0.3952 | 0.8940 |
| CO | R | 0.9913 | 0.9940 | 0.8720 | 0.8936 | 0.9943 | 0.9909 | 0.8890 | 0.9845 |
| | RMSE | 0.0105 | 0.0085 | 0.0813 | 0.0814 | 0.0093 | 0.0106 | 0.0814 | 0.0151 |
| | MAPE | 7.0901 | 6.4245 | 10.3984 | 10.3366 | 4.7962 | 6.8093 | 10.4436 | 9.7961 |
| | NSE | 0.8650 | 0.8909 | 0.8501 | 0.8518 | 0.8793 | 0.8628 | 0.8511 | 0.8047 |
| | KGE | 0.9380 | 0.9397 | 0.2570 | 0.2691 | 0.9135 | 0.9413 | 0.2640 | 0.9084 |
| $NO_x$ | R | 0.9972 | 0.9997 | 0.8801 | 0.8810 | 0.9987 | 0.999757 | 0.863657 | 0.994258 |
| | RMSE | 7.7129 | 2.4020 | 9.4919 | 9.4698 | 5.3896 | 2.15909 | 9.58474 | 11.31358 |
| | MAPE | 2.5449 | 1.0297 | 9.0727 | 9.8212 | 1.1279 | 0.883225 | 9.45723 | 6.856031 |
| | NSE | 0.9188 | 0.9747 | 0.1741 | 0.1743 | 0.9433 | 0.977281 | 0.173098 | 0.880954 |
| | KGE | 0.9338 | 0.9330 | 0.4478 | 0.4502 | 0.9303 | 0.93353 | 0.463115 | 0.91652 |
| HC | R | 0.9965 | 0.9872 | 0.7307 | 0.774439 | 0.9775 | 0.988969 | 0.694092 | 0.901939 |
| | RMSE | 0.8814 | 1.6023 | 8.3192 | 8.223366 | 2.2908 | 1.508026 | 8.362489 | 4.34556 |
| | MAPE | 7.5186 | 6.6204 | 9.1504 | 9.1796 | 8.8007 | 9.385357 | 9.8645 | 7.68846 |
| | NSE | 0.9117 | 0.8395 | 0.1669 | 0.176488 | 0.7706 | 0.848982 | 0.162556 | 0.564823 |
| | KGE | 0.9330 | 0.9403 | 0.4530 | 0.465161 | 0.9195 | 0.943125 | 0.39688 | 0.915195 |
| EGT | R | 0.9990 | 0.9992 | 0.8554 | 0.850462 | 0.9990 | 0.989444 | 0.844256 | 0.934189 |
| | RMSE | 1.5328 | 1.4330 | 5.1687 | 5.16444 | 1.5701 | 5.724247 | 5.21271 | 10.06475 |
| | MAPE | 0.5936 | 0.5248 | 10.9309 | 10.90522 | 0.8118 | 2.243228 | 10.20185 | 7.470471 |
| | NSE | 0.9554 | 0.9583 | 0.2682 | 0.268286 | 0.9543 | 0.833554 | 0.266882 | 0.620112 |
| | KGE | 0.9343 | 0.9338 | 0.5534 | 0.553829 | 0.9344 | 0.920852 | 0.549395 | 0.828652 |

Please cite this article in press as: Syed J, et al., Artificial Neural Network modeling of a hydrogen dual fueled diesel engine characteristics: An experiment approach, International Journal of Hydrogen Energy (2017), http://dx.doi.org/10.1016/j.ijhydene.2017.04.096

**Table B.4 – Benchmark indices in de-normalized form for six output parameter predictions for trainrp with different transfer function combinations.**

| Parameter | Benchmark Indices | Transfer function combination | | | | | | | |
|---|---|---|---|---|---|---|---|---|---|
| | | tansig–tansig | logsig–tansig | tansig–logsig | logsig–logsig | logsig–purelin | tansig–purelin | purelin–logsig | purelin–tansig |
| Number of neurons in hidden layer | | 20 | 10 | 10 | 6 | 9 | 11 | 13 | 9 |
| BTE | R | 0.9997 | 0.9998 | 0.9076 | 0.9206 | 0.9995 | 0.9996 | 0.9206 | 0.9997 |
| | RMSE | 0.2956 | 0.2494 | 4.9030 | 4.8324 | 0.2473 | 0.2349 | 4.8327 | 0.3590 |
| | MAPE | 1.0840 | 0.7782 | 5.8835 | 5.2252 | 0.9730 | 0.9525 | 7.2951 | 1.5270 |
| | NSE | 0.9636 | 0.9693 | 0.3956 | 0.4043 | 0.9695 | 0.9710 | 0.4043 | 0.9558 |
| | KGE | 0.9292 | 0.9318 | 0.5788 | 0.5941 | 0.9338 | 0.9334 | 0.5941 | 0.9236 |
| BSFC | R | 0.9990 | 0.9995 | 0.9513 | 0.9631 | 0.9997 | 0.9992 | 0.9499 | 0.9985 |
| | RMSE | 0.0090 | 0.0063 | 0.1694 | 0.1954 | 0.0045 | 0.0071 | 0.1694 | 0.0096 |
| | MAPE | 0.5801 | 0.6815 | 5.0837 | 6.8872 | 1.1063 | 1.3118 | 6.2954 | 1.2814 |
| | NSE | 0.9480 | 0.9635 | 0.0215 | 0.8286 | 0.9737 | 0.9591 | 0.0216 | 0.9447 |
| | KGE | 0.9308 | 0.9327 | 0.3672 | 0.6321 | 0.9337 | 0.9334 | 0.3795 | 0.9348 |
| CO | R | 0.9972 | 0.9963 | 0.8995 | 0.8995 | 0.9929 | 0.9967 | 0.9037 | 0.9844 |
| | RMSE | 0.0059 | 0.0068 | 0.0812 | 0.0812 | 0.0102 | 0.0065 | 0.0813 | 0.0143 |
| | MAPE | 4.2052 | 5.8000 | 9.5860 | 9.5878 | 5.2140 | 4.7516 | 10.4757 | 9.9924 |
| | NSE | 0.9244 | 0.9125 | 0.8482 | 0.8482 | 0.8684 | 0.9164 | 0.8498 | 0.8157 |
| | KGE | 0.9358 | 0.9359 | 0.2522 | 0.2520 | 0.9185 | 0.9357 | 0.2460 | 0.9367 |
| $NO_x$ | R | 0.9996 | 0.9994 | 0.8776 | 0.8852 | 0.9988 | 0.999862 | 0.828223 | 0.992926 |
| | RMSE | 3.0475 | 3.4097 | 8.3943 | 8.3730 | 5.0761 | 1.639013 | 8.8555 | 11.35723 |
| | MAPE | 1.2083 | 1.8680 | 5.4961 | 5.3255 | 1.8876 | 1.000897 | 5.10152 | 6.922218 |
| | NSE | 0.9679 | 0.9641 | 0.1751 | 0.1753 | 0.9466 | 0.982754 | 0.170249 | 0.880494 |
| | KGE | 0.9334 | 0.9333 | 0.4404 | 0.4376 | 0.9322 | 0.933405 | 0.447524 | 0.939387 |
| HC | R | 0.9938 | 0.9810 | 0.8567 | 0.842582 | 0.9912 | 0.990515 | 0.713735 | 0.900969 |
| | RMSE | 1.1918 | 2.1459 | 7.9913 | 7.99908 | 1.4287 | 1.45785 | 8.347304 | 4.338042 |
| | MAPE | 6.3279 | 11.7579 | 11.7136 | 11.8164 | 6.8907 | 12.14254 | 11.3116 | 11.56211 |
| | NSE | 0.8806 | 0.7851 | 0.1997 | 0.1989 | 0.8569 | 0.854007 | 0.164077 | 0.565576 |
| | KGE | 0.9351 | 0.8831 | 0.4096 | 0.4199 | 0.9298 | 0.93368 | 0.3819 | 0.880821 |
| EGT | R | 0.9128 | 0.9992 | 0.8516 | 0.8515 | 0.9974 | 0.999452 | 0.843419 | 0.930346 |
| | RMSE | 3.6427 | 1.4170 | 5.1545 | 5.1527 | 2.5225 | 1.153303 | 5.21051 | 11.24681 |
| | MAPE | 4.0762 | 0.6967 | 9.7722 | 9.7607 | 1.2138 | 0.643213 | 10.18999 | 6.654939 |
| | NSE | 0.5161 | 0.9588 | 0.2686 | 0.2686 | 0.9267 | 0.966465 | 0.266946 | 0.614818 |
| | KGE | 0.8812 | 0.9331 | 0.5538 | 0.5541 | 0.9361 | 0.933718 | 0.555384 | 0.942519 |

Please cite this article in press as: Syed J, et al., Artificial Neural Network modeling of a hydrogen dual fueled diesel engine characteristics: An experiment approach, International Journal of Hydrogen Energy (2017), http://dx.doi.org/10.1016/j.ijhydene.2017.04.096

**Table B.5 – Benchmark indices in de-normalized form for six output parameter predictions for traincgf with different transfer function combinations.**

| Parameter | Benchmark indices | Transfer function combination | | | | | | | |
|---|---|---|---|---|---|---|---|---|---|
| | | tansig–tansig | logsig–tansig | tansig–logsig | logsig–logsig | logsig–purelin | tansig–purelin | purelin–logsig | purelin–tansig |
| Number of neurons in hidden layer | | 10 | 12 | 11 | 9 | 13 | 8 | 5 | 3 |
| BTE | R | 0.9998 | 0.9998 | 0.9206 | 0.9205 | 0.9987 | 0.9997 | 0.9206 | 0.9221 |
| | RMSE | 0.2640 | 0.2029 | 4.8327 | 4.8324 | 0.4151 | 0.2012 | 4.8329 | 3.9832 |
| | MAPE | 1.0541 | 0.7543 | 9.2881 | 9.2404 | 1.3480 | 0.6152 | 10.3262 | 10.7317 |
| | NSE | 0.9675 | 0.9750 | 0.4043 | 0.4043 | 0.9488 | 0.9752 | 0.4042 | 0.5090 |
| | KGE | 0.9307 | 0.9333 | 0.5958 | 0.5936 | 0.9340 | 0.9335 | 0.5956 | 0.8112 |
| BSFC | R | 0.9977 | 0.7137 | 0.9496 | 0.9493 | 0.9988 | 0.9993 | 0.8471 | 0.9894 |
| | RMSE | 0.0211 | 0.2226 | 0.1692 | 0.1692 | 0.0088 | 0.0066 | 2.1954 | 2.0272 |
| | MAPE | 1.7471 | 4.1387 | 4.8317 | 4.8851 | 2.1190 | 1.1896 | 6.8872 | 3.7839 |
| | NSE | 0.8779 | 0.8856 | 0.0224 | 0.0224 | 0.9489 | 0.9619 | 0.7286 | 0.8430 |
| | KGE | 0.8916 | 0.8856 | 0.3825 | 0.3802 | 0.9341 | 0.9339 | 0.8065 | 0.9336 |
| CO | R | 0.9925 | 0.9951 | 0.8993 | 0.8992 | 0.9905 | 0.9980 | 0.9225 | 0.9795 |
| | RMSE | 0.0098 | 0.0083 | 0.0812 | 0.0812 | 0.0112 | 0.0051 | 0.0814 | 0.0158 |
| | MAPE | 4.3907 | 4.9002 | 9.5801 | 9.5770 | 6.3321 | 4.1370 | 10.7339 | 9.2863 |
| | NSE | 0.8740 | 0.8933 | 0.8482 | 0.8482 | 0.8551 | 0.9338 | 0.8511 | 0.7963 |
| | KGE | 0.9376 | 0.9301 | 0.2526 | 0.2525 | 0.9371 | 0.9343 | 0.2375 | 0.9335 |
| $NO_x$ | R | 0.9998 | 0.9987 | 0.8839 | 0.8729 | 0.9996 | 0.999243 | 0.829201 | 0.978659 |
| | RMSE | 1.8204 | 5.0838 | 8.3725 | 8.4289 | 2.7221 | 3.884286 | 8.86203 | 10.54112 |
| | MAPE | 0.9319 | 1.6137 | 5.3134 | 5.6193 | 1.2736 | 1.306773 | 5.15252 | 9.15744 |
| | NSE | 0.9808 | 0.9465 | 0.1753 | 0.1747 | 0.9714 | 0.959128 | 0.170181 | 0.678633 |
| | KGE | 0.9332 | 0.9338 | 0.4391 | 0.4417 | 0.9336 | 0.933872 | 0.453836 | 0.777556 |
| HC | R | 0.9906 | 0.9935 | 0.8499 | 0.847689 | 0.9906 | 0.968158 | 0.695882 | 0.898267 |
| | RMSE | 1.5112 | 1.2320 | 7.9856 | 8.01339 | 1.4240 | 2.7016 | 8.380978 | 4.756194 |
| | MAPE | 8.6644 | 3.4865 | 11.5821 | 11.1258 | 5.9507 | 6.419296 | 11.1511 | 10.12704 |
| | NSE | 0.8487 | 0.8766 | 0.2003 | 0.1975 | 0.8574 | 0.729454 | 0.160705 | 0.523701 |
| | KGE | 0.9258 | 0.9339 | 0.4194 | 0.4028 | 0.9371 | 0.933266 | 0.411617 | 0.912362 |
| EGT | R | 0.9962 | 0.9990 | 0.8404 | 0.8408 | 0.9983 | 0.987906 | 0.837047 | 0.911939 |
| | RMSE | 3.1733 | 1.5507 | 5.1899 | 5.1879 | 2.0304 | 5.415179 | 5.22315 | 9.88866 |
| | MAPE | 0.8674 | 0.4769 | 8.9446 | 8.9435 | 1.0785 | 2.525417 | 8.29198 | 8.596841 |
| | NSE | 0.9077 | 0.9549 | 0.2675 | 0.2676 | 0.9410 | 0.842541 | 0.266579 | 0.508923 |
| | KGE | 0.9342 | 0.9342 | 0.5575 | 0.5570 | 0.9351 | 0.945967 | 0.570162 | 0.936376 |

Please cite this article in press as: Syed J, et al., Artificial Neural Network modeling of a hydrogen dual fueled diesel engine characteristics: An experiment approach, International Journal of Hydrogen Energy (2017), http://dx.doi.org/10.1016/j.ijhydene.2017.04.096

**Table B.6 – Benchmark indices in de-normalized form for six output parameter predictions for trainscg with different transfer function combinations.**

| Parameter | Benchmark indices | Transfer function combination | | | | | | | |
|---|---|---|---|---|---|---|---|---|---|
| | | tansig–tansig | logsig–tansig | tansig–logsig | logsig–logsig | logsig–purelin | tansig–purelin | purelin–logsig | purelin–tansig |
| Number of neurons in hidden layer | | 9 | 11 | 12 | 18 | 20 | 17 | 4 | 2 |
| BTE | R | 0.9921 | 0.9996 | 0.9208 | 0.9206 | 0.9964 | 0.9979 | 0.9205 | 0.9996 |
| | RMSE | 1.1020 | 0.2541 | 4.8344 | 4.8324 | 0.7173 | 0.5318 | 4.8340 | 0.3097 |
| | MAPE | 2.1941 | 0.8753 | 9.4119 | 9.2354 | 2.7441 | 1.6056 | 9.3964 | 1.3098 |
| | NSE | 0.8641 | 0.9687 | 0.4041 | 0.4043 | 0.9116 | 0.9344 | 0.4041 | 0.9618 |
| | KGE | 0.9389 | 0.9319 | 0.6000 | 0.5940 | 0.9345 | 0.9350 | 0.5965 | 0.9331 |
| BSFC | R | 0.9980 | 0.9970 | 0.8331 | 0.9379 | 0.9867 | 0.9867 | 0.4161 | 0.9985 |
| | RMSE | 0.0113 | 0.0151 | 0.1739 | 0.1697 | 0.0318 | 0.0291 | 0.1954 | 0.0102 |
| | MAPE | 1.3066 | 1.3043 | 11.3544 | 10.2863 | 2.7367 | 3.2934 | 12.8867 | 0.7921 |
| | NSE | 0.9344 | 0.9127 | 0.8047 | 0.0199 | 0.8163 | 0.8321 | 0.1286 | 0.9411 |
| | KGE | 0.9352 | 0.9277 | 0.3525 | 0.3674 | 0.9037 | 0.9416 | 0.8663 | 0.9322 |
| CO | R | 0.9946 | 0.9951 | 0.9003 | 0.8992 | 0.9965 | 0.9701 | 0.8985 | 0.9847 |
| | RMSE | 0.0085 | 0.0077 | 0.0812 | 0.0812 | 0.0068 | 0.0201 | 0.0813 | 0.0143 |
| | MAPE | 6.2340 | 5.8453 | 9.6274 | 9.5782 | 5.5109 | 4.9455 | 10.4084 | 10.1400 |
| | NSE | 0.8907 | 0.9011 | 0.8482 | 0.8482 | 0.9127 | 0.7399 | 0.8501 | 0.8151 |
| | KGE | 0.9307 | 0.9383 | 0.2527 | 0.2526 | 0.9335 | 0.9347 | 0.2550 | 0.9332 |
| $NO_x$ | R | 0.9998 | 0.9995 | 0.8803 | 0.8851 | 0.9992 | 0.999934 | 0.877059 | 0.993971 |
| | RMSE | 2.1073 | 3.1663 | 8.3815 | 8.3725 | 4.1162 | 1.102053 | 8.50096 | 11.09111 |
| | MAPE | 0.9869 | 1.4962 | 5.4915 | 5.3129 | 2.1471 | 0.606441 | 5.00722 | 6.844404 |
| | NSE | 0.9778 | 0.9667 | 0.1752 | 0.1753 | 0.9567 | 0.988404 | 0.17398 | 0.883295 |
| | KGE | 0.9335 | 0.9336 | 0.4390 | 0.4385 | 0.9329 | 0.933387 | 0.445141 | 0.924908 |
| HC | R | 0.9824 | 0.9947 | 0.8721 | 0.815353 | 0.9917 | 0.978783 | 0.728669 | 0.901515 |
| | RMSE | 1.9077 | 1.0525 | 7.9934 | 8.194695 | 1.3498 | 2.053213 | 8.350974 | 4.336479 |
| | MAPE | 11.4530 | 8.0966 | 9.7119 | 9.5820 | 4.1711 | 11.14678 | 9.103 | 5.33101 |
| | NSE | 0.8090 | 0.8946 | 0.1995 | 0.1794 | 0.8648 | 0.794385 | 0.163709 | 0.565732 |
| | KGE | 0.9374 | 0.9339 | 0.4209 | 0.4425 | 0.9358 | 0.9557 | 0.371756 | 0.859991 |
| EGT | R | 0.9979 | 0.9979 | 0.8495 | 0.8515 | 0.9951 | 0.997175 | 0.840174 | 0.938801 |
| | RMSE | 2.3913 | 2.2988 | 5.1742 | 5.1524 | 3.5072 | 2.585175 | 5.21264 | 9.26188 |
| | MAPE | 1.1293 | 0.6227 | 9.9485 | 9.7435 | 1.3813 | 1.282015 | 10.21268 | 7.540639 |
| | NSE | 0.9305 | 0.9332 | 0.2680 | 0.2686 | 0.8980 | 0.92483 | 0.266884 | 0.643458 |
| | KGE | 0.9344 | 0.9354 | 0.5704 | 0.5543 | 0.9354 | 0.936307 | 0.560076 | 0.847008 |

Please cite this article in press as: Syed J, et al., Artificial Neural Network modeling of a hydrogen dual fueled diesel engine characteristics: An experiment approach, International Journal of Hydrogen Energy (2017), http://dx.doi.org/10.1016/j.ijhydene.2017.04.096

**Table B.7 – Benchmark indices in de-normalized form for six output parameter predictions for trainbfg with different transfer function combinations.**

| Parameter | Benchmark indices | Transfer function combination | | | | | | | |
|---|---|---|---|---|---|---|---|---|---|
| | | tansig–tansig | logsig–tansig | tansig–logsig | logsig–logsig | logsig–purelin | tansig–purelin | purelin–logsig | purelin–tansig |
| Number of neurons in hidden layer | | 8 | 20 | 8 | 11 | 7 | 6 | 7 | 4 |
| BTE | R | 0.9996 | 0.9994 | 0.9210 | 0.9209 | 0.9996 | 0.9997 | 0.9206 | 0.9997 |
| | RMSE | 0.3086 | 0.2944 | 4.8332 | 4.8362 | 0.2401 | 0.2037 | 4.8329 | 0.3241 |
| | MAPE | 1.3323 | 1.1809 | 6.3094 | 6.5174 | 0.7732 | 0.8489 | 6.3152 | 1.4454 |
| | NSE | 0.9620 | 0.9637 | 0.4042 | 0.4038 | 0.9704 | 0.9749 | 0.4042 | 0.9600 |
| | KGE | 0.9292 | 0.9337 | 0.5939 | 0.6033 | 0.9337 | 0.9334 | 0.5959 | 0.9268 |
| BSFC | R | 0.9968 | 0.9970 | 0.9458 | 0.9314 | 0.9996 | 0.9973 | 0.9501 | 0.9984 |
| | RMSE | 0.0177 | 0.0144 | 0.1697 | 0.1710 | 0.0047 | 0.0143 | 0.1694 | 0.0100 |
| | MAPE | 2.4796 | 0.9983 | 5.2823 | 5.7235 | 1.0807 | 1.7325 | 5.2981 | 1.0909 |
| | NSE | 0.8978 | 0.9169 | 0.0199 | 0.0125 | 0.9726 | 0.9173 | 0.0215 | 0.9420 |
| | KGE | 0.9208 | 0.9311 | 0.4034 | 0.3414 | 0.9337 | 0.9261 | 0.3853 | 0.9342 |
| CO | R | 0.9975 | 0.9973 | 0.8998 | 0.8573 | 0.9937 | 0.9963 | 0.9040 | 0.9845 |
| | RMSE | 0.0055 | 0.0060 | 0.0812 | 0.0910 | 0.0098 | 0.0067 | 0.0813 | 0.0143 |
| | MAPE | 3.9939 | 5.4955 | 6.6288 | 7.5574 | 4.2090 | 5.1769 | 7.4780 | 7.9908 |
| | NSE | 0.9291 | 0.9227 | 0.8482 | 0.8758 | 0.8740 | 0.9132 | 0.8498 | 0.8157 |
| | KGE | 0.9355 | 0.9343 | 0.2510 | 0.8652 | 0.9139 | 0.9369 | 0.2461 | 0.9343 |
| $NO_x$ | R | 0.9996 | 0.9995 | 0.8835 | 0.8815 | 0.9995 | 0.999837 | 0.876824 | 0.993581 |
| | RMSE | 2.8557 | 3.4647 | 8.3733 | 8.4054 | 3.8730 | 1.729667 | 8.49663 | 1.06199 |
| | MAPE | 1.3389 | 1.6152 | 5.3571 | 5.6213 | 1.1699 | 0.794861 | 5.03254 | 6.904353 |
| | NSE | 0.9700 | 0.9635 | 0.1753 | 0.1750 | 0.9592 | 0.9818 | 0.174026 | 0.883601 |
| | KGE | 0.9335 | 0.9312 | 0.4388 | 0.4359 | 0.9302 | 0.933494 | 0.440891 | 0.932483 |
| HC | R | 0.9868 | 0.9978 | 0.8119 | 0.857555 | 0.9849 | 0.9929 | 0.756315 | 0.90111 |
| | RMSE | 1.7429 | 0.6720 | 8.0630 | 8.032493 | 1.7323 | 1.239422 | 8.395823 | 4.425875 |
| | MAPE | 4.3480 | 6.8632 | 9.9714 | 9.8426 | 9.6382 | 10.03203 | 9.5332 | 9.14203 |
| | NSE | 0.8255 | 0.9327 | 0.1925 | 0.1956 | 0.8265 | 0.875881 | 0.159218 | 0.55678 |
| | KGE | 0.9311 | 0.9346 | 0.4109 | 0.4213 | 0.9492 | 0.932905 | 0.405694 | 0.949783 |
| EGT | R | 0.9995 | 0.9996 | 0.8511 | 0.8177 | 0.9933 | 0.998806 | 0.843401 | 0.935494 |
| | RMSE | 1.1403 | 0.9647 | 5.1532 | 5.2865 | 4.0192 | 1.772234 | 5.21051 | 8.34981 |
| | MAPE | 0.6521 | 0.5143 | 7.7779 | 7.4601 | 2.0908 | 0.963526 | 7.18993 | 7.085262 |
| | NSE | 0.9668 | 0.9719 | 0.2686 | 0.2647 | 0.8831 | 0.948468 | 0.266946 | 0.640901 |
| | KGE | 0.9338 | 0.9334 | 0.5550 | 0.5619 | 0.9370 | 0.933683 | 0.55545 | 0.893313 |

Please cite this article in press as: Syed J, et al., Artificial Neural Network modeling of a hydrogen dual fueled diesel engine characteristics: An experiment approach, International Journal of Hydrogen Energy (2017), http://dx.doi.org/10.1016/j.ijhydene.2017.04.096

## REFERENCES

[1] Varde K, Frame G. Hydrogen aspiration in a direct injection type diesel engine-its effects on smoke and other engine performance parameters. Int J Hydrogen Energy 1983;8(7):549–55.
[2] Mathur H, Das L, Patro T. Hydrogen fuel utilization in CI engine powered end utility systems. Int J Hydrogen Energy 1992;17(5):369–74.
[3] Masood M, Ishrat M, Reddy A. Computational combustion and emission analysis of hydrogen–diesel blends with experimental verification. Int J Hydrogen Energy 2007;32(13):2539–47.
[4] Lata D, Misra A, Medhekar S. Effect of hydrogen and LPG addition on the efficiency and emissions of a dual fuel diesel engine. Int J Hydrogen Energy 2012;37(7):6084–96.
[5] Cho Y, Song S, Chun K. Hydrogen effects on diesel combustion and emissions with an LPL-EGR system. Int J Hydrogen Energy 2013;38(23):9897–906.
[6] Santoso W, Bakar R, Nur A. Combustion characteristics of diesel-hydrogen dual fuel engine at low load. Energy Procedia 2013;32:3–10.
[7] De Morais A, Mendes Justino M, Valente O, Hanriot S, Sodré J. Hydrogen impacts on performance and $CO_2$ emissions from a diesel power generator. Int J Hydrogen Energy 2013;38(16):6857–64.
[8] Zhou J, Cheung C, Leung C. Combustion, performance, regulated and unregulated emissions of a diesel engine with hydrogen addition. Appl Energy 2014;126:1–12.
[9] Parlak A, Islamoglu Y, Yasar H, Egrisogut A. Application of artificial neural network to predict specific fuel consumption and exhaust temperature for a diesel engine. Appl Therm Eng 2006;26:824–8.
[10] Yusaf TF, Buttsworth DR, Saleh KH, Yousif BF. CNG-diesel engine performance and exhaust emission analysis with the aid of artificial neural network. Appl Energy 2010;87:1661–9.
[11] Uzun A. A parametric study for specific fuel consumption of an intercooled diesel engine using a neural network. Fuel 2012;93:189–99.
[12] Bietresato M, Calcante A, Mazzetto F. A neural network approach for indirectly estimating farm tractors engine performances. Fuel 2015;143:144–54.
[13] Chen Y, McCall T, Baichwal A, Meyer M. The application of an artificial neural network and pharmacokinetic simulations in the design of controlled-release dosage forms. J Control Release 1999;59(1):33–41.
[14] Basheer I, Hajmeer M. Artificial neural networks: fundamentals, computing, design, and application. J Microbiol Methods 2000;43(1):3–31.
[15] Sun Y, Peng Y, Chen Y, Shukla A. Application of artificial neural networks in the design of controlled release drug delivery systems. Adv Drug Deliv Rev 2003;55(9):1201–15.
[16] Çay Y, Çiçek A, Kara F, Sağiroğlu S. Prediction of engine performance for an alternative fuel using artificial neural network. Appl Therm Eng 2012;37:217–25.
[17] Taghavifar H, Taghavifar H, Mardani A, Mohebbi A, Khalilarya S. A numerical investigation on the wall heat flux in a DI diesel engine fueled with n-heptane using a coupled CFD and ANN approach. Fuel 2015;140:227–36.
[18] Mohamed Ismail H, Ng H, Queck C, Gan S. Artificial neural networks modelling of engine-out responses for a light-duty diesel engine fuelled with biodiesel blends. Appl Energy 2012;92:769–77.
[19] Sompop J, Sathaporn C, Prateep C. Effect of hydrogen addition on diesel engine operation and NOx emission: a thermodynamic study. Am J Appl Sci 2012;9(9):1472–8.
[20] Szwaja S, Grab-Rogalinski K. Hydrogen combustion in a compression ignition diesel engine. Int J Hydrogen Energy 2009;34(10):4413–21.
[21] Jhang S, Chen K, Lin S, Lin Y, Cheng W. Reducing pollutant emissions from a heavy-duty diesel engine by using hydrogen additions. Fuel 2016;172:89–95.
[22] Bose P, Maji D. An experimental investigation on engine performance and emissions of a single cylinder diesel engine using hydrogen as inducted fuel and diesel as injected fuel with exhaust gas recirculation. Int J Hydrogen Energy 2009;34(11):4847–54.
[23] Deb M, Sastry G, Bose P, Banerjee R. An experimental study on combustion, performance and emission analysis of a single cylinder, 4-stroke DI-diesel engine using hydrogen in dual fuel mode of operation. Int J Hydrogen Energy 2015;40(27):8586–98.
[24] Karagöz Y, Güler İ, Sandalcı T, Yüksek L, Dalkılıç A. Effect of hydrogen enrichment on combustion characteristics, emissions and performance of a diesel engine. Int J Hydrogen Energy 2016;41(1):656–65.
[25] Patro T. Combustion study of hydrogen fueled DI diesel engine: simplified heat release analysis. Int J Hydrogen Energy 1993;18(3):231–41.
[26] Lilik G, Zhang H, Herreros J, Haworth D, Boehman A. Hydrogen assisted diesel combustion. Int J Hydrogen Energy 2010;35(9):4382–98.
[27] Hamdan M, Selim M, Al-Omari S, Elnajjar E. Hydrogen supplement co-combustion with diesel in compression ignition engine. Renew Energy 2015;82:54–60.
[28] Heywood J. Internal combustion engine fundamentals. 1st ed. New York, N.Y: McGraw-Hill; 1988.
[29] An H, Yang W, Maghbouli A, Li J, Chou S, Chua K. A numerical study on a hydrogen assisted diesel engine. Int J Hydrogen Energy 2013;38(6):2919–28.
[30] Samuel S, McCormick G. Hydrogen enriched diesel combustion. In: SAE technical paper; 2010.
[31] Velmurugan K, Sathiyagnanam A. Impact of antioxidants on NOx emissions from a mango seed biodiesel powered DI diesel engine. Alex Eng J 2016;55(1):715–22.
[32] Majumder U, Chakraborti P, Banerjee R, Debbarma B. Experimental study on the role of ethanol on performance emission trade-off and tribological characteristics of a CI engine. Renew Energy 2016;86:972–84.
[33] Chintala V, Subramanian K. CFD analysis on effect of localized in-cylinder temperature on nitric oxide (NO) emission in a compression ignition engine under hydrogen-diesel dual-fuel mode. Energy 2016;116:470–88.
[34] Chauhan B, Kumar N, Cho H. A study on the performance and emission of a diesel engine fueled with Jatropha biodiesel oil and its blends. Energy 2012;37(1):616–22.
[35] Torres García M, José Jiménez-Espadafor Aguilar F, Sánchez Lencero T. Experimental study of the performances of a modified diesel engine operating in homogeneous charge compression ignition (HCCI) combustion mode versus the original diesel combustion mode. Energy 2009;34(2):159–71.
[36] Senthil Kumar M, Ramesh A, Nagalingam B. Use of hydrogen to enhance the performance of a vegetable oil fuelled compression ignition engine. Int J Hydrogen Energy 2003;28(10):1143–54.
[37] Talibi M, Hellier P, Balachandran R, Ladommatos N. Effect of hydrogen-diesel fuel co-combustion on exhaust emissions with verification using an in–cylinder gas sampling technique. Int J Hydrogen Energy 2014;39(27):15088–102.
[38] Senthil Kumar M, Jaikumar M. Studies on the effect of hydrogen induction on performance, emission and

Please cite this article in press as: Syed J, et al., Artificial Neural Network modeling of a hydrogen dual fueled diesel engine characteristics: An experiment approach, International Journal of Hydrogen Energy (2017), http://dx.doi.org/10.1016/j.ijhydene.2017.04.096

combustion behaviour of a WCO emulsion based dual fuel engine. Int J Hydrogen Energy 2014;39(32):18440–50.
[39] Deb M, Paul A, Debroy D, Sastry G, Panua R, Bose P. An experimental investigation of performance-emission trade off characteristics of a CI engine using hydrogen as dual fuel. Energy 2015;85:569–85.
[40] Banerjee R, Debbarma B, Roy S, Chakraborti P, Bose P. An experimental investigation on the potential of hydrogen–biohol synergy in the performance-emission trade-off paradigm of a diesel engine. Int J Hydrogen Energy 2016;41(5):3712–39.
[41] Paul A, Bose P, Panua R, Banerjee R. An experimental investigation of performance-emission trade off of a CI engine fueled by diesel–compressed natural gas (CNG) combination and diesel–ethanol blends with CNG enrichment. Energy 2013;55:787–802.
[42] Armitage P, Colton T. Encyclopedia of biostatistics. 1st ed. Chichester, West Sussex, England: John Wiley; 2005.

## Nomenclature

$CV_D$: Lower calorific value of Diesel (kJ/kg)
$I$: Current generated by AC dynamometer (amp)
$M_D$: Mass flow rate of Diesel (kg/s)
$n$: number of trial cases
$O_i$: output for ith trial case
$T_i$: target for ith trial case
$V$: Voltage generated by AC dynamometer (V)
$M_{H_2}$: Mass flow rate of $H_2$ (kg/s)
$CV_{H_2}$: Lower calorific value of $H_2$ (kJ/kg)
$\sigma_T$: Standard deviation of targets of ANN
$\sigma_O$: Standard deviation of outputs of ANN
$\alpha$: Relative variability ratio ($\sigma_O/\sigma_T$)
$\beta$: Ratio of mean of outputs to mean of targets
$\gamma$: The Pearson Product Moment correlation coefficient (Covariance/ $\sigma_T * \sigma_O$)

Please cite this article in press as: Syed J, et al., Artificial Neural Network modeling of a hydrogen dual fueled diesel engine characteristics: An experiment approach, International Journal of Hydrogen Energy (2017), http://dx.doi.org/10.1016/j.ijhydene.2017.04.096